

‘This introductory textbook goes beyond the descriptive level and the usual engineering approximations to a deeper, yet accessible, level of fundamental composite mechanics that provides valuable insights into composite performance.’

William Curtin, École polytechnique fédérale de Lausanne

This fully expanded and updated edition provides both scientists and engineers with all the information they need to understand composite materials, covering their underlying science and technological usage.

Key features include:

- 4 completely new chapters on surface coatings, highly porous materials, bio-composites and nano-composites
- Thoroughly revised chapters on fibres and matrices, the design, fabrication and production of composites, mechanical and thermal properties and industry applications, all while retaining the structure and conceptual framework of previous editions
- Extensively expanded and restructured referencing
- Increased coverage of background science, including the manipulation of stresses and strains as second-rank tensors, and fracture mechanics
- A consistent framework of nomenclature and notation
- A comprehensive set of homework questions, with model answers available online, explaining how calculations associated with the properties of composite materials should be tackled, as well as access to educational software at doitpoms.ac.uk

This is an excellent, self-contained text, designed primarily for final-year undergraduates in materials science and engineering, but also for graduate students and researchers in both academia and industry.

T. W. CLYNE is Professor of Mechanics of Materials in the Department of Materials Science and Metallurgy at the University of Cambridge, and the Director of the Gordon Laboratory. He is also the Director of DoITPoMS, an educational materials science website, a Fellow of the Royal Academy of Engineering and a Helmholtz International Fellow.

D. HULL is an Emeritus Professor at the University of Liverpool. He is also a Fellow of the Royal Society and a Fellow of the Royal Academy of Engineering.

MRS MATERIALS RESEARCH SOCIETY®
Advancing materials. Improving the quality of life.

Cover illustration: Stress and strain fields in a transverse section of a polyester-40vol%glass long fibre composite (Courtesy of Dr. M. Burley)

CAMBRIDGE
UNIVERSITY PRESS
www.cambridge.org



Clyne and Hull
An Introduction to Composite Materials
THIRD EDITION

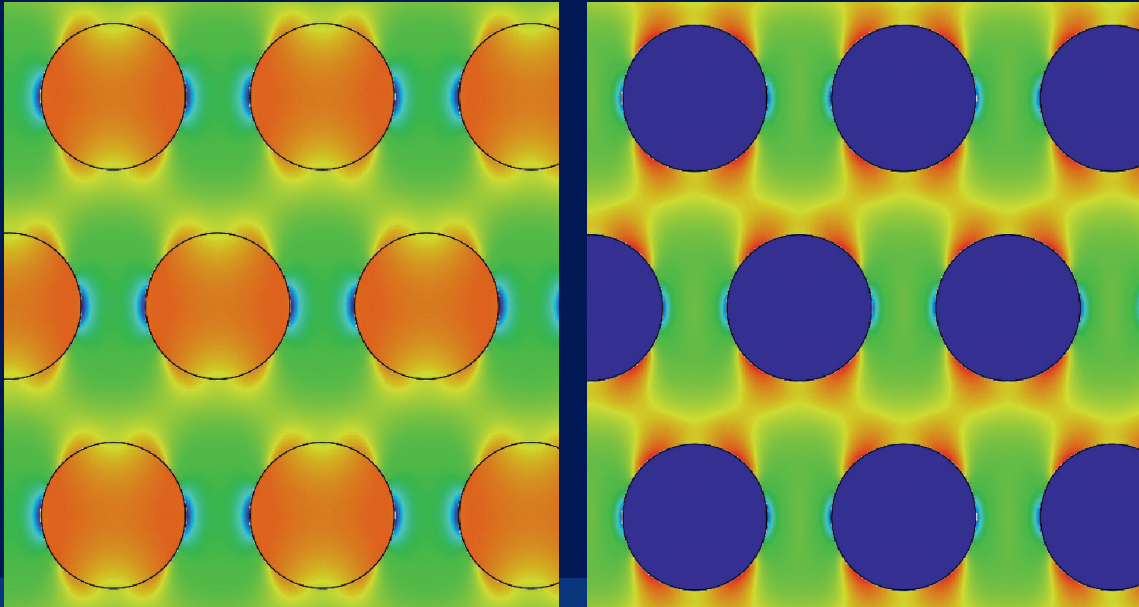
MRS®

CAMBRIDGE

An Introduction to Composite Materials

THIRD EDITION

T. W. Clyne and D. Hull



CAMBRIDGE

MRS MATERIALS RESEARCH SOCIETY®
Advancing materials. Improving the quality of life.

‘This introductory textbook goes beyond the descriptive level and the usual engineering approximations to a deeper, yet accessible, level of fundamental composite mechanics that provides valuable insights into composite performance.’

William Curtin,
École polytechnique fédérale de Lausanne

‘Composite materials combine and comprise an understanding of materials science, mechanics and general engineering.

The 3rd edition of *An Introduction to Composite Materials* by T. W. Clyne and D. Hull is a carefully revised version of the previous very successful textbook. It is a comprehensive summary of the current knowledge in composites science and technology – specially prepared as a textbook for young scientists and graduate students to get a substantial insight into this still young area.

I personally recommend this book to my graduate students.’

Karl Schulte,
Technische Universität Hamburg

‘This extensively revised and expanded edition includes the latest developments in composites research and applications. The new chapters on surface coatings, highly porous materials and bio- and nano-composites are uniquely valuable.’

Tsu-Wei Chou,
University of Delaware

An Introduction to Composite Materials

Third Edition

This fully expanded and updated edition provides both scientists and engineers with all the information they need to understand composite materials, covering their underlying science and technological usage. It includes four completely new chapters on surface coatings, highly porous materials, bio-composites and nano-composites, as well as thoroughly revised chapters on fibres and matrices, the design, fabrication and production of composites, mechanical and thermal properties and industry applications. Extensively expanded referencing engages readers with the latest research and industrial developments in the field, and increased coverage of essential background science makes this a valuable self-contained text. A comprehensive set of homework questions, with model answers available online, explains how calculations associated with the properties of composite materials should be tackled, and educational software accompanying the book is available at doitpoms.ac.uk.

This is an invaluable text for final-year undergraduates in materials science and engineering, and graduate students and researchers in academia and industry.

T. W. Clyne is Professor of Mechanics of Materials in the Department of Materials Science and Metallurgy at the University of Cambridge, and the Director of the Gordon Laboratory. He is also the Director of DoITPoMS, an educational materials science website, a Fellow of the Royal Academy of Engineering and a Helmholtz International Fellow.

D. Hull is an Emeritus Professor at the University of Liverpool. He is also a Fellow of the Royal Society and a Fellow of the Royal Academy of Engineering.

An Introduction to Composite Materials

Third Edition

T. W. CLYNE

University of Cambridge

D. HULL

University of Liverpool

 MATERIALS RESEARCH SOCIETY®
Advancing materials. Improving the quality of life.

 CAMBRIDGE
UNIVERSITY PRESS

CAMBRIDGE

UNIVERSITY PRESS

University Printing House, Cambridge CB2 8BS, United Kingdom

One Liberty Plaza, 20th Floor, New York, NY 10006, USA

477 Williamstown Road, Port Melbourne, VIC 3207, Australia

314-321, 3rd Floor, Plot 3, Splendor Forum, Jasola District Centre, New Delhi - 110025, India

79 Anson Road, #06-04/06, Singapore 079906

Cambridge University Press is part of the University of Cambridge.

It furthers the University's mission by disseminating knowledge in the pursuit of education, learning and research at the highest international levels of excellence.

www.cambridge.org

Information on this title: www.cambridge.org/9780521860956

DOI: 10.1017/9781139050586

First and Second editions © Cambridge University Press 1981, 1996.

Third edition © T. W. Clyne and D. Hull 2019

This publication is in copyright. Subject to statutory exception and to the provisions of relevant collective licensing agreements, no reproduction of any part may take place without the written permission of Cambridge University Press.

First published 1981

Second edition 1996

Third edition 2019

A catalogue record for this publication is available from the British Library

Library of Congress Cataloging in Publication data

Names: Clyne, T. W., author. | Hull, Derek, author.

Title: An introduction to composite materials / T.W. Clyne (University of Cambridge), D. Hull (University of Liverpool).

Description: Cambridge ; New York, NY : Cambridge University Press, [2019] |

Includes bibliographical references and index.

Identifiers: LCCN 2018061490 | ISBN 9780521860956 (hardback : alk. paper)

Subjects: LCSH: Composite materials.

Classification: LCC TA418.9.C6 H85 2019 | DDC 620.1/18–dc23

LC record available at <https://lccn.loc.gov/2018061490>

ISBN 978-0-521-86095-6 Hardback

Additional resources for this publication at www.cambridge.org/compositematerials

Cambridge University Press has no responsibility for the persistence or accuracy of URLs for external or third-party internet websites referred to in this publication, and does not guarantee that any content on such websites is, or will remain, accurate or appropriate.

Contents

	<i>Preface to the Third Edition</i>	page ix
	<i>Nomenclature</i>	xi
1	General Introduction	1
	1.1 Types of Composite Material	1
	1.2 Property Maps and Merit Indices for Composite Systems	4
	1.3 The Concept of Load Transfer	7
	References	8
2	Fibres, Matrices and Their Architecture in Composites	9
	2.1 Reinforcements	9
	2.2 Statistics of Fibre Tensile Strength	17
	2.3 Matrices	20
	2.4 Long Fibre Composite Architectures	23
	2.5 Short Fibre Configurations	25
	References	28
3	Elastic Deformation of Long Fibre Composites	31
	3.1 Axial Young's Modulus	31
	3.2 Transverse Young's Modulus	33
	3.3 Other Elastic Constants	37
	References	42
4	Tensor Analysis of Anisotropic Materials and the Elastic Deformation of Laminae	43
	4.1 Tensor Representation of Elastic Deformation	43
	4.2 Stress–Strain Relationships and Engineering Constants	53
	4.3 Off-Axis Elastic Constants of Laminae	56
	References	66
5	Elastic Deformation of Laminates	67
	5.1 Loading of a Stack of Plies	67
	5.2 Stresses and Distortions in Laminates	71

6	Stresses and Strains in Short Fibre and Particulate Composites	77
	6.1 The Shear Lag Model	77
	6.2 The Eshelby Method	89
	References	95
7	The Interface Region	97
	7.1 Bonding Mechanisms	97
	7.2 Experimental Measurement of Bond Strength	102
	7.3 Controlling the Interfacial Bond Strength	108
	References	111
8	Stress-Based Treatment of the Strength of Composites	114
	8.1 Failure Modes and Strength of Long Fibre Composites	114
	8.2 Failure of Laminæ under Off-Axis Loads	122
	8.3 Strength of Laminates	128
	8.4 Failure of Tubes and Pipes under Internal Pressure	135
	References	139
9	Fracture Mechanics and the Toughness of Composites	142
	9.1 Fracture Mechanics	142
	9.2 Fracture of Composite Materials	151
	9.3 Sub-Critical Crack Growth in Composites	168
	References	173
10	Thermal Effects in Composites	178
	10.1 Thermal Expansion and Thermal Stresses	178
	10.2 Thermal Cycling Effects	186
	10.3 Time-Dependent Deformation (Creep and Viscous Flow)	192
	10.4 Thermal Conduction	201
	References	216
11	Surface Coatings as Composite Systems	220
	11.1 Curvature in Substrate–Coating Systems	220
	11.2 Curvatures and Their Measurement in Real Systems	227
	11.3 Spallation (Interfacial Debonding) of Coatings	232
	References	235
12	Highly Porous Materials as Composite Systems	238
	12.1 Types of Highly Porous Material and Their Production	238
	12.2 Mechanical Properties of Highly Porous Materials	244
	12.3 Permeation of Fluids through Highly Porous Materials	255
	12.4 Thermal Properties of Highly Porous Materials	260
	References	263

13	Bio-Composites and Recycling	268
	13.1 Biomaterials as Composite Systems	268
	13.2 Cellulose-Based Fibres and Composites	271
	13.3 Ceramic-Based Bio-Composites	277
	13.4 Recycling of Composite Materials	281
	References	283
14	Scale Effects and Nano-Composites	286
	14.1 Scale Effects in Composite Systems	286
	14.2 Fine-Scale, Carbon-Based Reinforcement	289
	14.3 Composites Containing Nano-Scale Reinforcement	293
	References	298
15	Fabrication of Composites	301
	15.1 Polymer Matrix Composites	301
	15.2 Metal Matrix Composites	306
	15.3 Ceramic Matrix Composites	311
	References	315
16	Applications of Composites	319
	16.1 Overview of Composite Usage	319
	16.2 Aerospace and Automotive Applications	320
	16.3 Marine and Wind Energy Applications	324
	16.4 Sports Goods	325
	16.5 High-Temperature Applications	327
	References	330
	<i>Appendix: Questions</i>	333
	<i>Index</i>	342

Preface to the Third Edition

The topic of composite materials continues to evolve in terms of range, research activity and technological importance. This was the case between publication of the first edition in 1981 and the second in 1996. The coverage of the book was expanded and broadened to reflect this. In fact, the rate of development of composites has accelerated in the period since then and hence a further substantial enlargement and evolution in coverage has been implemented. Composites certainly now constitute one of the most important and diverse classes of material. All materials scientists and engineers need to be familiar with at least the main principles and issues involved in their usage.

While this edition retains much of the structure and conceptual framework of the previous two editions, it now includes four completely new chapters. Moreover, all of the other chapters, which progressively cover the various types of fibre and matrix, the structure of composites, their elastic deformation, strength and toughness, the role of the interface and the thermal characteristics of composite systems, have all been rewritten, to a greater or lesser extent. There has, of course, been extensive updating to reflect the prodigious levels of research and industrial development in the area over the past couple of decades. The citation of references has been expanded and restructured. While previously there was a short list of sources for further information at the end of each chapter (with limited specific citation in the text), this edition provides much more comprehensive referencing, both in quantity and in terms of detail. This change is designed to improve the potential value to researchers, as well as undergraduates.

Nevertheless, much of the material remains pitched at around the level of a final-year undergraduate or a Masters course. In fact, another innovation in this edition is the provision of a large number of questions (with model answers available on the website). Many of these are derived from a third-year undergraduate course on composite materials that has been running (and evolving!) for over 30 years in the Materials Science Department at Cambridge University. A further pedagogical development concerns educational software packages that can be used in conjunction with the book. These form part of a major initiative called DoITPoMS (Dissemination of IT for the Promotion of Materials Science), hosted on the Cambridge University site (www.doitpoms.ac.uk), which comprises a large number of interactive modules covering a wide range of topics. Many are relevant to the general area of composite materials, but several are specific to topics in the book and reference to them is included in the enhanced coverage.

In addition to this expansion in terms of the range of teaching resources, attempts have been made to encompass more of the necessary background science, so as to

reduce the need to consult other texts. Examples of this include more comprehensive coverage of the manipulation of stresses and strains as (second-rank) tensors, which is particularly important when treating highly anisotropic materials such as composites, and a considerably expanded chapter on fracture mechanics. These are both areas in which the background knowledge needed for a full understanding of the behaviour of composites is relatively demanding. Bringing this material within the remit of the book is aimed at creating a more coherent overall picture, within a consistent framework of nomenclature and symbolism.

In addition, the new chapters are aimed at expansion of the range of situations that can usefully be treated using the approaches of composite theory. The first of these (Chapter 11) concerns the mechanics of substrate/coating systems, a topic of considerable scientific and technological interest. It is shown how tools developed within the framework of the book can be used to obtain insights into the development of curvature in such systems, and also into the driving forces for spallation (debonding) of such coatings. The following chapter, on highly porous materials, is based on a similar philosophy – in this case showing how such materials, which are also of technological importance, can usefully be treated as special types of composite material.

Chapter 13 is also a new addition. This concerns bio-composites, such as wood and bone. Of course, these are widely recognised as (complex) composite materials, and the treatment presented here is fairly superficial. Nevertheless, information is presented on how they relate to manufactured composites, and there is some coverage of the important topics of recycling, degradation and sustainability. The final new chapter relates to scale effects in composites and to the class of materials sometimes referred to as nano-composites. Despite the enormous levels of interest and research in such materials over recent decades, levels of industrial exploitation have remained minimal – at least as far as load-bearing components are concerned. The reasons for this are outlined.

The final two chapters, as in the previous edition, concern fabrication of composites and their application. These are largely in the form of case histories of various types. There has again been considerable expansion and updating of these, reflecting the huge range of current industrial usage and the ways in which composites have penetrated numerous markets – and in many cases facilitated their expansion and raised their significance. There is extensive cross-reference in these chapters to locations in the book where details are provided about characteristics of the composites concerned that have favoured their usage.

Finally, we would again like to thank our wives, Gail and Pauline, for their invaluable support during the preparation of this book.

T. W. Clyne and D. Hull
November 2018

Nomenclature

Parameters

A	(m^2)	cross-sectional area
A	($\text{s}^{-1} \text{Pa}^{-n}$)	constant in creep equation (10.17)
a	($-$)	direction cosine
a	(m)	radius of sphere
a	($\text{m}^2 \text{s}^{-1}$)	thermal diffusivity
b	(m)	width
Bi	($-$)	Biot number
C	(Pa)	stiffness (tensor of fourth rank)
C	($\text{Pa}^{-n} \text{s}^{-m-1}$)	constant in creep equation (10.18)
c	($\text{J K}^{-1} \text{m}^{-3}$)	volume specific heat
c	(m)	crack length or flaw size
c	($-$)	$\cos(\phi)$
D	(m)	fibre diameter
d	(m)	fibre/particle diameter
E	(Pa)	Young's modulus
E'	(Pa)	biaxial modulus
e	($-$)	relative displacement
f	($-$)	reinforcement (fibre) volume fraction
F	(N)	force
G	(J m^{-2})	strain energy release rate
G	(Pa)	shear modulus
g	($-$)	fraction (undergoing pull-out)
H	(m)	thickness (of substrate)
h	(m)	thickness (of coating)
h	(m)	spacing between fibres
h	(m)	height
h	($\text{W m}^{-2} \text{K}^{-1}$)	heat transfer coefficient
I	($-$)	unit tensor (identity matrix)
I	($-$)	invariant (in the secular equation)
I	(m^4)	second moment of area
K	(Pa)	bulk modulus
K	($\text{Pa m}^{1/2}$)	stress intensity

K	(W m ⁻¹ K ⁻¹)	thermal conductivity
k	(J K ⁻¹)	Boltzmann's constant
L	(m)	sample length
L	(m)	fibre half-length
M	(m N)	bending moment
m	(-)	Weibull modulus
N	(mole ⁻¹)	Avogadro's number
N	(-)	number of loading cycles
N	(m ⁻²)	number of fibres per unit area
n	(-)	dimensionless constant
n	(-)	stress exponent
P	(N)	force
P	(Pa)	pressure
P	(-)	probability
P	(-)	porosity
Q	(m ³ m ⁻² s ⁻¹)	fluid flux
q	(W m ⁻²)	heat flux
R	(J K ⁻¹ mole ⁻¹)	universal gas constant
R	(m)	far-field radial distance from fibre axis
r	(m)	radius of fibre, tube or crack tip
S	(Pa ⁻¹)	compliance tensor
S	(-)	Eshelby tensor
S	(Pa)	stress amplitude during fatigue
S	(m ² m ⁻³)	specific surface area
s	(-)	fibre aspect ratio ($2L/d = L/r$)
s	(-)	sin(ϕ)
T	(K)	absolute temperature
T	(N m)	torque
T'	(K m ⁻¹)	thermal gradient
t	(m)	ply or wall thickness
t	(s)	time
U	(J)	work done during fracture
u	(m)	displacement in x direction (fibre axis)
V	(m ³)	volume
v	(m s ⁻¹)	velocity
W	(J m ⁻³)	work of fracture
x	(m)	distance (Cartesian coordinate)
y	(m)	distance (Cartesian coordinate)
z	(m)	distance (Cartesian coordinate)
α	(K ⁻¹)	thermal expansion coefficient
β	(-)	reinforcement/matrix ratio conductivity ratio
β	(-)	dimensionless constant
Δ	(-)	relative change in volume

δ	(m)	crack opening displacement
δ	(m)	pull-out length
δ	(m)	distance from neutral axis to interface
ε	(–)	strain
ϕ	(°)	loading angle (between fibre axis and loading direction)
Φ	(°)	global loading angle (between laminate reference axis and loading direction)
γ	(–)	shear strain
γ	(J m ⁻²)	surface energy
η	(–)	interaction ratio
η	(–)	dimensionless constant
η	(Pa s)	viscosity
κ	(m ⁻¹)	curvature
κ	(m ²)	(specific) permeability
λ	(m)	mean free path
λ	(–)	dimensionless constant
θ	(û)	wetting angle
ν	(–)	Poisson ratio
ρ	(kg m ⁻³)	density
ρ	(m)	distance from fibre axis
Σ	(N m ²)	beam stiffness
σ	(Pa)	stress
τ	(Pa)	shear stress
ψ	(°)	phase angle (mode mix)
ζ	(–)	dimensionless constant

Subscripts

0	initial
1	x direction (along fibre axis)
2	y direction
3	z direction
A	applied
a	air
b	background
b	buckling
c	coated
c	composite
c	critical
d	debonding
e	fibre end
f	failure
f	fibre (reinforcement)

fr	frictional sliding
g	global
H	hoop
H	hydrostatic
i	interfacial
k	kink band
L	liquid
m	matrix
n	network
p	pull-out
p	particle
r	radial
s	survival
RoM	rule of mixtures
t	stress transfer
th	threshold
trans	transverse
u	failure (ultimate tensile)
u	uncoated
v	volume
Y	yield (0.2% proof stress often taken)
θ	hoop
*	critical (e.g. debonding or fracture)

Superscripts

ax	axial
C	constrained
T	transformation
T*	misfit
tr	transverse

1 General Introduction

The usage of composite materials continues to expand rapidly. The current world-wide market value is not easy to estimate, but is certainly more than US\$100 billion. Composites now constitute one of the broadest and most important classes of engineering materials – second only to steels in industrial significance and range of applications. There are several reasons for this. One is that they often offer highly attractive combinations of stiffness, strength, toughness, lightness and corrosion resistance. Another is that there is considerable scope for tailoring their structure to suit service conditions. This concept is well illustrated by biological materials such as wood, bone, teeth and hide, which are all composites with complex internal structures that have been designed (via evolutionary processes) to give mechanical properties well suited to the performance requirements. This versatility is, of course, attractive for many industrial purposes, although it also leads to complexity that needs to be well understood if they are to be used effectively. In fact, adaptation of manufactured composite structures for different engineering purposes requires input from several branches of science. In this introductory chapter, an overview is given of the types of composites that have been developed.

1.1 Types of Composite Material

Many materials are effectively composites. This is particularly true of natural biological materials, which are often made up of at least two constituents. In many cases, a strong and stiff component is present, often in elongated form, embedded in a softer and more compliant constituent forming the *matrix*. For example, wood is made up of fibrous chains of cellulose molecules in a matrix of lignin, while bone and teeth are both essentially composed of hard inorganic crystals (hydroxy-apatite or osteones) in a matrix of a tough organic constituent called collagen. Many of the complexities of the structure and properties of bone are well illustrated in the extensive work of Currey [1,2] and a brief survey of biological composites is presented later in this book (Chapter 13).

Commonly, such composite materials show marked *anisotropy* – that is to say, their properties vary significantly when measured in different directions. This usually arises because the harder (and stiffer) constituent is in fibrous form, with the fibre axes preferentially aligned in particular directions. In addition, one or more of the constituents may exhibit inherent anisotropy as a result of their crystal structure. In natural materials, such anisotropy of mechanical properties is often exploited within the structure. For example, wood is much stronger in the direction of the fibre tracheids,

which are usually aligned parallel to the axis of the trunk or branch, than it is in the transverse directions. High strength is required in the axial direction, since a branch becomes loaded like a cantilevered beam by its own weight and the trunk is stressed in a similar way by the action of the wind. Such beam bending causes high stresses along the length, but not through the thickness.

In making artificial composite materials, this potential for controlled anisotropy offers considerable scope for integration between the processes of material specification and component design. This is an important point about use of composites, since it represents a departure from conventional engineering practice. An engineer designing a component commonly takes material properties to be isotropic. In fact, this is often inaccurate even for conventional materials. For example, metal sheet usually has different properties in the plane of the sheet than those in the through-thickness direction, as a result of *crystallographic texture* (preferred orientation) produced during rolling, although such variations are in many cases relatively small. In a composite material, on the other hand, large anisotropies in stiffness and strength are possible and must be taken into account during design. Not only must variations in strength with direction be considered, but the effect of any anisotropy in stiffness on the stresses created in the component under external load should also be taken into account. The material can thus be produced bearing in mind the way it will be loaded when it is made into a component, with the processes of material production and component manufacture being integrated into a single operation. This happens when biological materials are produced. In fact, the fine-scale structure of a natural material such as wood is often influenced during its creation by stresses acting on it at the time.

There are several different types of composite. Examples of possible configurations with different types of reinforcement are shown in Fig. 1.1. The matrix material may be polymeric, metallic or ceramic, although by far the largest proportion of composites in

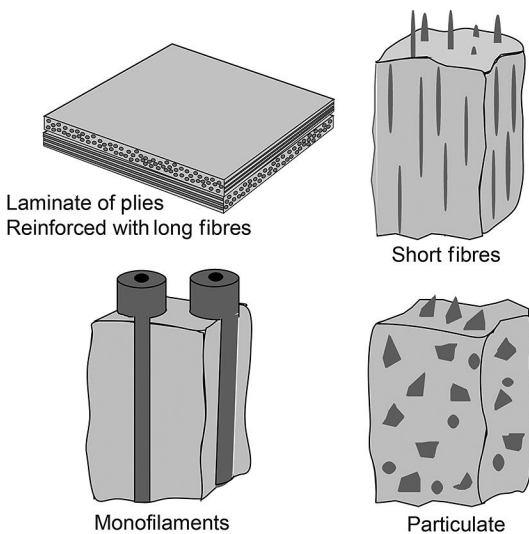


Fig. 1.1 Schematic depiction of different types of reinforcement configuration.

industrial use are based on polymers – predominantly thermosets (resins), although in some cases thermoplastics are used. Reinforcements are usually ceramics of some sort, most commonly long fibres of carbon or glass. It should, however, be appreciated that other types of fibre, including polymeric and metallic forms, are used in commercial composite materials and that there are also materials containing short fibres or particulate reinforcement. Composites with metallic or ceramic matrices (MMCs and CMCs) are also of industrial significance. Furthermore, it should be noted that there is extensive ongoing research into novel types of composite. As might be expected, property enhancements sought by the introduction of reinforcement into metals or ceramics are often less pronounced than those for polymers, with improvements in high-temperature performance or tribological properties often of interest for MMCs. With CMCs, on the other hand, the objective is usually to enhance the toughness of the matrix. With all three types of matrix, there is enormous potential for achieving property combinations that are unobtainable in monolithic materials.

In considering the formulation of a composite material for a particular type of application, a starting point is clearly to consider the properties exhibited by the potential constituents. Properties of particular interest include the stiffness (Young's modulus), strength and toughness. Density is also of great significance in many situations, since the mass of the component may be of critical importance. Thermal properties, such as expansivity and conductivity, must also be taken into account. In particular, because composite materials are subject to temperature changes (during manufacture and/or in service), a mismatch between the thermal expansivities of the constituents leads to internal residual stresses. These can have a strong effect on the mechanical behaviour.

Some indicative property data are shown in Table 1.1 for a few engineering materials, including some composites. These values are very approximate, but they immediately confirm that some attractive property combinations (for example, high stiffness/strength/toughness, in combination with low density) can be obtained with

Table 1.1 Overview of properties of some engineering materials, including composites.

Material	Density ρ (kg m^{-3})	Young's modulus E (GPa)	Tensile strength σ_s (MPa)	Fracture energy G_c (kJ m^{-2})	Thermal conductivity K ($\text{W m}^{-1} \text{K}^{-1}$)	Thermal expansivity α ($\mu\text{ε K}^{-1}$)
Mild steel	7800	208	400	100	40	17
Concrete	2400	40	20	0.01	2	12
Spruce (// to grain)	600	16	80	4	0.5	3
Spruce (\perp to grain)	600	1	2	0.2	0.3	10
Chopped strand mat (in-plane)	1800	20	300	30	8	20
Carbon fibre composite (// to fibres)	1600	200	1500	10	10	0
Carbon fibre composite (\perp to fibres)	1600	10	40	0.2	2	30
Al-20% SiC _p (MMC)	2800	90	300	2	140	18

composites. They also, of course, highlight the potential significance of anisotropy in the properties of certain types of composite. An outline of how such properties can be predicted from those of the individual constituents forms a key part of the contents of this book.

1.2 Property Maps and Merit Indices for Composite Systems

Selecting the constituents and structure of a composite material for a particular application is not a simple matter. The introduction of reinforcement into a matrix alters all of its properties (assuming that the volume fraction, f , can be regarded as significant, which usually means more than a few per cent). It may also be necessary to take account of possible changes in the microstructure of the matrix resulting from the presence of the reinforcement. The generation of residual stresses (for example, from differential thermal contraction during manufacture) may also be significant. Before considering such secondary effects, it is useful to take a broad view of the property combinations obtainable with different composite systems. This can be visualised using *property maps*. Two examples are presented in Fig. 1.2. These shows plots of: (a) Young's modulus, E ; and (b) hardness,¹ H , against density, ρ . A particular material (or type of material) is associated with a point or a region in such maps. This is a convenient method of comparing the property combinations offered by potential matrices and reinforcements with those of alternative conventional materials.

Of course, in general, attractive combinations of these two pairs of properties will lie towards the top-left of these diagrams, although in the case of hardness it should be appreciated that this is a relatively complex 'property' that depends to some extent on microstructure (whereas both stiffness and density are more or less independent of microstructure for a particular type of material). Once the properties of a particular type of composite have been established, then they can, of course, be included in maps of this type. An example is shown in Fig. 1.3, which compares approximate combinations of E and ρ expected for some composite materials with those for materials such as steel, titanium and alumina.

This concept can often be taken a little further by identifying a *merit index* for the performance required, in the form of a specified combination of properties. Appropriate models can then be used to place upper and lower bounds on the composite properties involved in the merit index, for a given volume fraction of reinforcement. The framework for such manipulations was set out in Ashby's seminal work [3], which he also oriented specifically towards composites [4]. An example is shown in Fig. 1.4 for three different fibres and a polymer matrix. The shaded areas joining the points corresponding

¹ Hardness is not really a 'genuine' property, although it is a measure of the resistance that the material offers to plastic deformation and is related to the yield stress, σ_Y , and the work-hardening characteristics. It is obtained from the size of an indent produced by an applied load. This is a simple and quick procedure, but hardness values vary with indenter shape and load, since these affect the plastic strains induced. If work-hardening is neglected, then the (Vickers) hardness is expected to have a value of around $3\sigma_Y$.

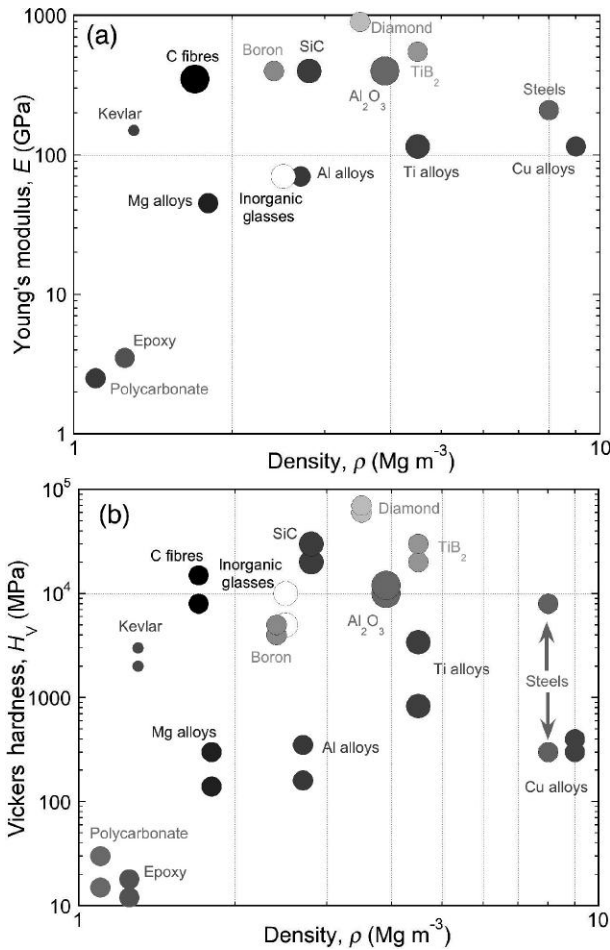


Fig. 1.2 Maps of (a) stiffness and (b) hardness against density, for a selection of metals, ceramics and polymers.

to a fibre to that of the matrix (epoxy resin) represent the possible combinations of E and ρ obtainable from a composite of the two constituents concerned. (The density of a composite is given simply by the weighted mean of the constituents; the stiffness, however, can only be identified as lying between upper and lower bounds – see Chapter 4 – unless more information is given about fibre orientation.) As can be seen in the figure, it is also possible to carry out this operation with the ‘reinforcement’ being holes – i.e. to consider the creation of foams. As with fibres, the architecture of the porosity is important, and could be such as to cause anisotropy.

Also shown in Fig. 1.4 are lines corresponding to constant values of the ratios E/ρ , E/ρ^2 and E/ρ^3 . These ratios represent the merit indices to be maximised to obtain minimum component weight consistent with a maximum permissible deflection for different component shapes and loading configurations. For example, the lightest square

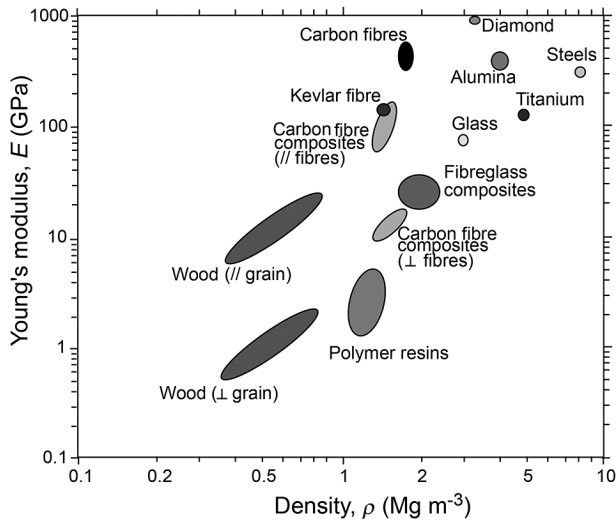


Fig. 1.3 Map of stiffness against density for some common materials, including some fibres and composites.

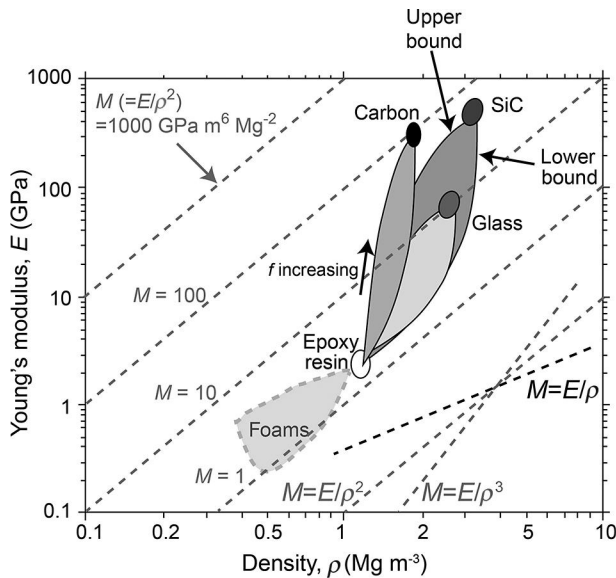


Fig. 1.4 Predicted map of stiffness against density for composites of glass, carbon or SiC fibres in a matrix of epoxy resin. Also shown is the effect of introducing porosity (to create foams). The shaded areas are bounded by the axial and transverse values of E predicted for these composite systems. The diagonal dotted lines represent constant values of three merit indices (E/ρ , E/ρ^2 and E/ρ^3). For E/ρ^2 , several lines are shown corresponding to different values of the ratio.

section beam able to support a given load without exceeding a specified deflection is the one made of the material with the largest value of E/ρ^2 . It can be seen from the figure that, while the introduction of carbon and silicon carbide fibres would improve the E/ρ ratio in similar fashions, carbon fibres would be much the more effective of the two if the ratio E/ρ^3 were the appropriate merit index. Also notable is that a foam could perform better (i.e. give a lighter component capable of bearing a certain type of load) than the monolithic matrix, particularly if the loading configuration is such that the merit index is E/ρ^3 .

1.3 The Concept of Load Transfer

Central to an understanding of the mechanical behaviour of a composite is the concept of *load-sharing* between the matrix and the reinforcing phase. The stress may vary sharply from point to point (particularly with short fibres or particles as reinforcement), but the proportion of the external load borne by each of the individual constituents can be gauged by volume-averaging the load within them. Of course, at equilibrium, the external load must equal the sum of the volume-averaged loads borne by the constituents (e.g. the matrix and the fibre).² This gives rise to the condition

$$f\bar{\sigma}_f + (1 - f)\bar{\sigma}_m = \sigma_A \quad (1.1)$$

governing the volume-averaged matrix and fibre stresses ($\bar{\sigma}_m, \bar{\sigma}_f$) in a composite under an external applied stress σ_A , containing a volume fraction f of reinforcement. Thus, for a simple two-constituent composite under a given applied load, a certain proportion of that load will be carried by the fibres and the remainder will be carried by the matrix. Provided the response of the composite remains elastic, this proportion will be independent of the applied load and it represents an important characteristic of the material. It depends on the volume fraction, shape and orientation of the reinforcement and on the elastic properties of both constituents. The reinforcement may be regarded as acting efficiently if it carries a relatively high proportion of the externally applied load. This can result in higher strength, as well as greater stiffness, because the reinforcement is usually stronger, as well as stiffer, than the matrix. Analysis of the load-sharing that occurs in a composite is central to an understanding of the mechanical behaviour of composite materials.

The above concept constitutes an important criterion for distinguishing between a genuine composite and a material in which there is an additional constituent – for example, there might be a fine dispersion of a precipitate – that is affecting the properties (such as the yield stress and hardness), but is present at too low a volume fraction to carry a significant proportion of an applied load.

² In the absence of an externally applied load, the individual constituents may still be stressed (due to the presence of residual stresses), but these must balance each other according to Eqn (1.1).

References

1. Currey, JD, The many adaptations of bone. *Journal of Biomechanics* 2003; **36**: 1487–1495.
2. Currey, JD, The structure and mechanics of bone. *Journal of Materials Science* 2012; **47**: 41–54.
3. Ashby, MF, *Materials Selection in Mechanical Design*. Pergamon Press, 1992.
4. Ashby, MF, Criteria for selecting the components of composites: overview No. 106. *Acta Metallurgica et Materialia* 1993; **41**: 1313–1335.

2 Fibres, Matrices and Their Architecture in Composites

In this chapter, an overview is provided of the types of fibre and matrix in common use and of how they are assembled into composites. Many types of reinforcement, mostly fibres, are available commercially. Their properties are related to atomic structure and the presence of defects, which must be controlled during manufacture. Matrices may be based on polymers, metals or ceramics. Choice of matrix is usually related to required properties, component geometry and method of manufacture. Certain composite properties may be sensitive to the nature of the reinforcement/matrix interface; this topic is covered in Chapter 7. Properties are also dependent on the arrangement and distribution of fibres, i.e. the fibre architecture, an expression that encompasses intrinsic features of the fibres, such as their diameter and length, as well as their volume fraction, alignment and spatial distribution. Fibre arrangements include laminae (sheets containing aligned long fibres) and laminates that are built up from these. Other continuous fibre systems, such as woven configurations, are also covered. Short fibre systems can be more complex and methods of characterising them are also briefly described.

2.1 Reinforcements

Many reinforcements are available, some designed for particular matrix systems. The reader is referred below to more specialised publications for details about their production, structure and properties. Nevertheless, an overview of certain characteristics is useful here and this is provided in Table 2.1 for a range of fibres in common use. Most of these have relatively high stiffness and low density. Carbon, glass and, to some extent, aramid fibres (such as *Kevlar*) are used extensively in polymer matrix composites. Ceramic fibres (and particles) can be used to reinforce metals, while both metallic and ceramic fibres are commonly used in ceramic-based composites. The latter include *carbon-carbon* composites, which sound a little unlikely, but are in fact of considerable importance for applications such as aircraft brakes – see Section 16.5.1.

Among the points to note in this table is that some fibres are highly anisotropic in certain properties (such as stiffness), although for most purposes the axial properties are much more important than those in other directions. It may also be noted that the tensile strength data are very approximate. This is unavoidable, since the fracture strength of ceramic (brittle) materials is sensitive to the presence of flaws in the sample concerned.

Table 2.1 Overview of diameters and properties of several different types of fibre.

Fibre	Density ρ (kg m^{-3})	Axial modulus E_1 (GPa)	Transverse modulus E_2 (GPa)	Shear modulus G_{12} (GPa)	Poisson ratio ν_{12}	Axial strength σ_s (GPa)	Axial CTE α_1 ($\mu\text{ε K}^{-1}$)	Transverse CTE α_2 ($\mu\text{ε K}^{-1}$)
E-glass ($d \sim 10 \mu\text{m}$)	2600	76	76	31	0.22	3–4	5	5
Kevlar ($d \sim 12 \mu\text{m}$)	1470	150	4	3	0.35	2–3	–4	54
HS (PAN) carbon ($d \sim 8 \mu\text{m}$)	1750	250–300	14	14	0.20	3–6	–1	10
HM (PAN) carbon ($d \sim 8 \mu\text{m}$)	1940	400–800	6	78	0.20	2–4	–1	10
SiC monofilament ($d \sim 150 \mu\text{m}$)	3200	400	400	170	0.20	3	5	5
SiC whisker ($d \sim 0.5 \mu\text{m}$)	3200	550	350	170	0.17	6	4	4
α Al_2O_3 long ($d \sim 10 \mu\text{m}$)	3900	385	385	150	0.26	2	8	8
δ Al_2O_3 staple ($d \sim 3 \mu\text{m}$)	3400	300	300	120	0.26	2	8	8
Stainless steel (304) ($d \sim 50\text{--}500 \mu\text{m}$)	7800	200	200	80	0.27	1	17	17
Tungsten ($d \sim 50\text{--}500 \mu\text{m}$)	19 300	413	413	155	0.28	3	5	5
Flax ($\sim 65\%$ cellulose) ($d \sim 50 \mu\text{m}$)	1500	80	10	10	0.3	2	–	–

In fact, the relatively high values for many of these strengths (relative to what might be expected for corresponding bulk material) is largely due to the fact that (fine) fibres tend to contain very few large flaws.

2.1.1 Carbon Fibres

Carbon fibres are largely composed of graphene planes oriented so that they lie parallel to the axis of the fibre. Apart from this condition, and a tendency for a number of adjacent planes to lie parallel to each other, the arrangement is rather disordered. It is illustrated [1] in Fig. 2.1. Such an arrangement is often referred to as ‘turbostratic’, a term used to describe a structure in which basal planes have slipped out of alignment. The details of the structure do depend on the way the fibres are produced, but the key point is that graphene has very strong bonding within the plane, so the alignment in carbon fibres ensures that the axial stiffness and strength are high.¹ (The in-plane Young’s modulus of a perfect graphene crystal, normal to the c -axis, is ~ 1000 GPa,

¹ There has been considerable interest in making ‘micro-fibrils’ from carbon nanotubes (since it is very difficult to produce composites with significant volume fractions of well-dispersed nanotubes); however, the structure of large assemblies of nanotubes is likely to resemble that of conventional turbostratic carbon fibre and indeed stiffness and strength values of such micro-fibrils have tended to be no higher than those of standard carbon fibre – see Chapter 14.

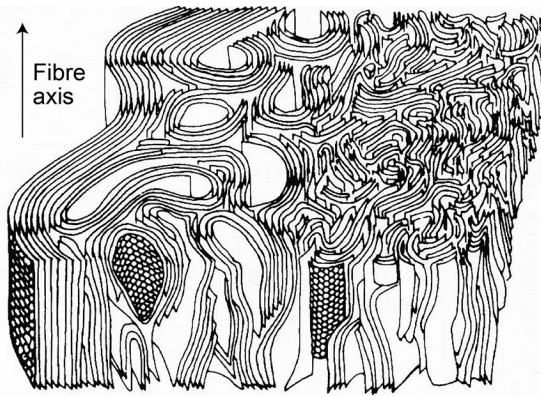


Fig. 2.1 Schematic representation of the (turbostratic) structure of a carbon fibre [1].

while that along the c -axis is only ~ 35 GPa.) Carbon fibres are thus highly anisotropic, not only in stiffness and strength, but also in properties such as thermal expansivity (which is higher transversely) and thermal conductivity (which is higher in the axial direction). Their thermal properties are described in Sections 10.1.1 and 10.3.1. For many purposes, this anisotropy is not very significant. For example, the design of fibre composites is often such that applied loads are borne primarily along fibre axes. (In fact, under transverse loading of a uniaxial composite, its stiffness and strength are in any event low, since the matrix, which is usually weak and compliant, bears much of the load, so that fibre stiffness and strength in that direction is unimportant.)

The detailed structure of carbon fibres can vary significantly, depending on exactly how they are made. There are two main processing routes, which are briefly outlined below. An overview [2] of the key properties (stiffness and tensile strength) for these two types of commercial product can be seen in Fig. 2.2, although it should be noted that these data are from the manufacturers (and might hence be slightly optimistic in some cases). It is clear from this plot that there is, in general, a choice between *high modulus* (HM) or *high strength* (HS) products. Use of lower processing temperatures leads to somewhat less dense products that are strong, but not so stiff, while higher temperatures give higher density and stiffness, but accompanied by greater brittleness (lower strains to failure and lower strength).

From PolyAcryloNitrile (PAN)

PAN-based carbon fibres date from around 1960 and are now in extensive use, with annual production of over 60 000 tonnes. PAN resembles polyethylene, but with one of the two hydrogen atoms on every other carbon backbone atom replaced by a nitrile ($-\text{C}\equiv\text{N}$) group. Bulk PAN is drawn down to a fibre and stretched to produce alignment of the molecular chains. When the stretched fibre is heated, the nitrile groups react to produce a *ladder polymer*, consisting of rows of six-membered rings. While the fibre is still under tension, it is heated in an oxygen-containing environment. This causes further chemical reaction and the formation of cross-links between the ladder molecules.

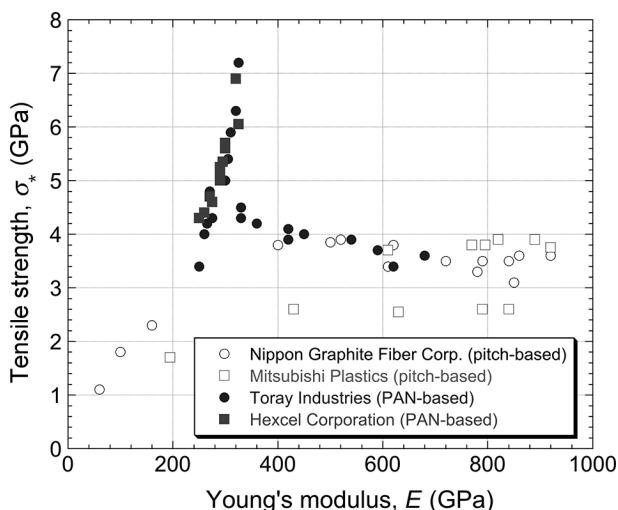


Fig. 2.2 Fibre strength as a function of modulus for commercially available carbon fibres (taken from manufacturers' pamphlets [2]).

The oxidised PAN is then reduced to give the carbon ring structure, which is converted to turbostratic graphite by heating at higher temperatures (in the absence of air – i.e. *pyrolysing*). The fibres usually have a thin skin of circumferential basal planes and a core with randomly oriented crystallites. Detailed information about PAN fibres is available in the literature [2,3].

From Mesophase Pitch

This process originated in the mid-1960s and, while these fibres are less extensively used than PAN-derived variants, they are still of considerable commercial significance. Pitch, which occurs naturally, is a complex mixture of thousands of different species of hydrocarbon and heterocyclic molecules. When heated above 350°C, condensation reactions occur, creating large, flat molecules that tend to align parallel to one another. This is often termed '*mesophase pitch*', a viscous liquid exhibiting local molecular alignment (i.e. a *liquid crystal*). This liquid is extruded through a multi-hole spinneret to produce 'green' yarn, which is made infusible by oxidation at temperatures below its softening point. These fibres can be converted thermally, without applied tension, into a graphitic fibre with a high degree of axial preferred orientation. The basal planes are often oriented radially, as well as being aligned along the fibre axis. This conversion is carried out at ~2000°C. The resulting structures are highly graphitic – more so than for PAN fibres. This affects some thermo-physical properties. For example, the Young's modulus is often high (~700–800 GPa), as is the thermal conductivity (~1000 W m⁻¹ K⁻¹). This latter feature is advantageous for certain applications, such as the carbon–carbon composites used for aircraft brakes (Section 16.5.1). The tensile strength, on the other hand, is usually only moderate (~2–4 GPa). Several publications provide detailed coverage of pitch-based carbon fibres [4,5]

2.1.2 Glass Fibres

Glass fibres are used for many different purposes. Most of them are based on silica (SiO_2), with additions of oxides such as those of calcium, boron, sodium, iron and aluminium. The atomic-scale structure is amorphous. The main building block is SiO_4 tetrahedra. A key issue is the extent to which what would, in the case of quartz (pure silica) glass, be a rigid network of these tetrahedra gets disrupted by the presence of 'network-modifying' (lower valence) oxides, such as Na_2O . Such additions reduce the glass transition temperature, so that the material is easier to deform (draw) at relatively low temperatures, although of course this has the effect of reducing the maximum use temperature. Other properties, such as stiffness, are also affected by the composition, although only to a limited degree. Many different compositions are in use, but most fibres used in making composites are of a type designated *E-glass*, which has a combination of properties that is well-suited to this application.

Glass fibres are produced by melting the raw materials in a reservoir and feeding into a series of platinum bushings, each of which has several hundred holes in its base. The glass flows under gravity and fine filaments are drawn mechanically downwards as the glass extrudes from the holes. The fibres are wound onto a drum at speeds of several thousand metres per minute. Control of the fibre diameter is achieved by adjusting the head of the glass in the tank, the viscosity of the glass (dependent on composition and temperature), the diameter of the holes and the winding speed. The diameter of *E-glass* is usually between 8 and 15 μm .

The structure, and hence the properties, of glass are isotropic. A key property is, of course, the tensile strength. As for all brittle materials, this depends on the presence of flaws, which are predominantly located at the surface. All brittle fibres tend to get stronger as their diameter is reduced, since this is naturally associated with having finer flaws. On the other hand, various practical difficulties arise if the diameter becomes very small (sub-micron) – see Chapter 14 – and a value in the vicinity of 10 μm is popular. This tends to offer a good combination of strength and flexibility – i.e. such fibres can be handled (usually as bundles of some sort) easily and safely. Freshly drawn *E-glass* fibres have very few surface flaws and their tensile strength is high (~3–4 GPa). However, they are rather susceptible to the accidental introduction of surface damage, and hence to a sharp reduction in strength. In fact, very high fibre strength is not necessarily required for good composite properties: in addition to stiffness, the toughness of a composite is a key property in terms of its engineering usage, and this is more sensitive to issues related to the interface and to the promotion of energy-absorbing mechanisms such as fibre pull-out – see Chapter 9. Nevertheless, a fibre strength that is at least fairly high is likely to be useful and it is certainly helpful to ensure that its surface is protected from mechanical damage and chemical attack, both during fibre handling and *in situ* in the composite material.

To minimise such damage, fibres for use in composites are usually treated with a *size* at an early stage in manufacture. This is a thin coating applied by spraying the fibres with water containing an emulsified polymer. The size actually serves several purposes: not only does it protect the surface from damage, but it also helps hold the fibres

together during handling and promotes bonding with the matrix in the composite – i.e. it acts as a *coupling agent*. This is considered further in Section 7.3.1, although the reader is referred to other publications [6–8] for the details of glass fibre production, including treatment with a size.

2.1.3 Polymeric Fibres

Fibres containing long-chain (polymeric) molecules are of considerable significance for use in composite materials, particularly if *cellulose* (in wood and other natural materials) is included in this category. The most important polymeric fibre for use in manufactured composites is the aromatic polyamide (*aramid*) that is produced under the trade name *Kevlar*. In fact, the structures of cellulose and Kevlar, shown in Fig. 2.3, are rather similar. Both have phenyl rings in the backbone and hydrogen bonding between adjacent chains. Chain alignment is produced in Kevlar during drawing and stretching operations, giving it an axial modulus of ~150 GPa. As for carbon fibres, the transverse stiffness is much lower. One characteristic of polymeric fibres, in contrast to glass and carbon, is that they tend to be relatively tough. This is because their failure often involves at least some plastic deformation, associated with a degree of sliding between chains. While this sounds like an important attribute, in practice composite materials often have a high toughness, which is not dependent on the inherent toughness of the fibre (or of the matrix) – see Chapter 9. Nevertheless, there are some applications for which relatively tough fibres offer a distinct advantage. A good example of this is bullet-proof vests, which commonly contain Kevlar fibres. On the other hand, polymeric fibres do have limitations, including a relatively low stiffness and also very limited tolerance of heat. Details about the production and structure of aramid fibres are available in the literature [9,10].

Certain other polymeric fibres are of commercial importance (although not used very widely in composite materials). These include polyethylene and nylon. These are not usually very stiff, but they do have fairly high tensile strengths and they are cheap

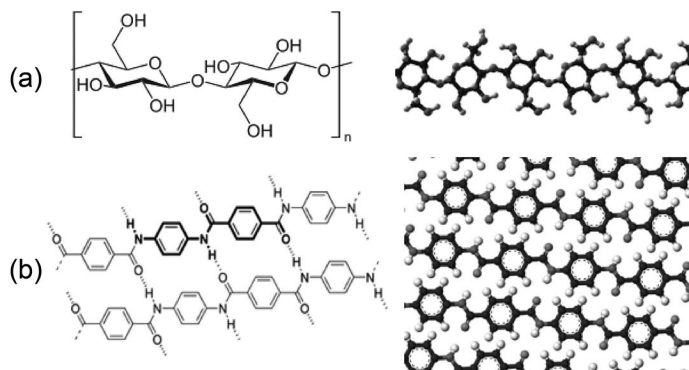


Fig. 2.3 Structures of (a) cellulose and (b) Kevlar (polyparaphenylene terephthalamide) molecules.

and easy to produce. There is also a wide range of natural composites – mostly reinforced by cellulose fibres, which are formed by *in situ* polymerisation of glucose molecules. Cellulose fibres (micro-fibrils) can be extracted from a range of plants, such as cotton, flax and jute, as well as timber [11]. It can be seen from the data for flax in Table 2.1 that the properties of cellulose fibres compare fairly well with those of many artificial fibres, particularly if density is important. Some manufactured composites are based on such fibres. Bio-composites, and also certain recycling issues, are covered in Chapter 13.

2.1.4 Silicon Carbide

Other reinforcements are used in composites, although at much lower levels than carbon and glass fibres. These include silicon carbide, which has a similar structure to diamond and offers a similarly attractive combination of low density and high stiffness, combined with good thermal stability and thermal conductivity. It is much easier to synthesise than diamond and can readily be produced in large quantities in a crude form such as powder. Bulk production of fibres is more problematic. Several different forms have been developed, although it should be appreciated that none of these are currently in very extensive commercial use.

Large-diameter (~100–150 µm) fibres, often termed *monofilaments*, are made by chemical vapour deposition (CVD) onto fine core fibre substrates, usually carbon (~30 µm diameter) or tungsten (~10 µm diameter). The core fibre is fed continuously through a reaction chamber. A gaseous carbon-containing silane, such as methyl-trichloro-silane (CH_3SiCl_3), is passed through the chamber. The core fibre is heated, usually by passing an electrical current through it, and the gas dissociates thermally at the fibre surface to deposit the SiC. Surface layers, designed to improve the resistance to handling damage and the compatibility with the matrix (usually a metal, intermetallic or ceramic), are often deposited in a second reactor. For example, graphitic layers are commonly applied. The process is also employed commercially for production of boron fibres. Details are available elsewhere concerning both fibre production [12] and use of Ti-based composites containing this type of reinforcement [13].

Fibres that are primarily SiC are made by a polymer precursor route analogous to the PAN-based method for carbon fibres (Section 2.1.1). Fibres about 15 µm in diameter are produced in this way, using *polycarbosilane* (PCS) as a precursor. The best-known fibre produced by this route, which has the trade name *Nicalon*, was first developed in the late 1970s, although it has been further developed since then. Polycarbosilane is produced in a series of chemical steps involving the reaction of dichlorodimethylsilane with sodium to produce polydimethylsilane, which yields polycarbosilane on heating in an autoclave. This is spun into fibres, which are then pyrolysed at temperatures up to 1300°C. The final product contains significant levels of SiO_2 and free carbon, as well as SiC. These fibres thus tend to have inferior properties to the (much purer) monofilaments, although their smaller diameter means they are much more flexible and easier to handle (as bundles), as well as being somewhat cheaper. Details of their production, structure, properties and usage (in ceramic matrix composites) are available elsewhere [14,15].

2.1.5 Oxide Fibres

Oxide fibres offer potential for good resistance to oxidative degradation, which is often a problem for other fibres when used at high temperature (in metal- or ceramic matrix composites). Those in widest use are predominantly combinations of alumina and silica. Fibres containing approximately 50% of each of these (i.e. aluminosilicates) comprise by far the greatest tonnage of refractory fibres and are in extensive use for high-temperature insulation purposes. Such fibres are usually glassy. Alumina fibres with much lower silica contents, which are crystalline, are more expensive to manufacture, but have greater resistance to high temperature and higher stiffness and strength [16].

Both continuous and short alumina fibres are available. An example of the former type is the 'FP' fibre (20 μm diameter) produced by Du Pont [17], while the latter group includes the 'Saffil' fibre (3 μm diameter), which was originally marketed as a replacement for asbestos but has since been investigated quite extensively as a reinforcement in metal matrix composites (MMCs). However, commercial usage of both types remains relatively limited.

2.1.6 Ceramic Whiskers and Nanotubes

There has been extensive interest in fine-scale (sub-micron) reinforcement for composites, mostly in the form of single crystals. This started some considerable time ago (in the 1950s), when it became clear that various ceramics (and metals) can be grown (often from the vapour phase) in the form of elongated single crystals, usually termed *whiskers*. Since these are so fine (perhaps around 100 nm in diameter), and have no grain boundaries, they often have very high strengths. Of course, these are not easy to measure, but they certainly can be of the order of 6–8 GPa, which is probably starting to approach the theoretical limit (corresponding to atomic planes shearing over one another, without dislocations being present; this can only be estimated, but it is around 3–5% of the shear modulus). Such strength values have caused considerable excitement over the years, recently reanimated with the intense interest in carbon nanotubes, which are similar in concept, but even finer (approximately a few nanometres in diameter). There has certainly been a lot of work on production of whiskers (particularly SiC and Si_3N_4 [18–20]) and carbon nanotubes [21,22].

However, this has not, so far, led to commercially viable composites. This topic is covered in more detail in Chapter 14, but the main difficulties are clear. One of the problems is that such fine fibres are expensive to produce, and also difficult to handle – partly because they readily become airborne and are then a potential health hazard. It is also very difficult to disperse significant levels of ultra-fine fibres within a matrix. Moreover, and more fundamentally, the key properties of composites containing such ultra-fine reinforcement are unlikely to be attractive, despite their high tensile strength values. In particular, the toughness of the composite is likely to be relatively low with very fine reinforcement. This issue is covered in Chapter 9.

2.1.7 Particulate

Particles are attractive in some respects as reinforcement, and, while they are quite commonly single crystals and can be relatively fine, they constitute a distinctly different category from the previous one. Powder particles offer advantages in terms of cost and ease of handling and processing. Such material is in fact used in a wide variety of composite materials, often simply as a cheap filler. For example, many engineering polymers and rubbers contain additions of powders such as talc, clays, mica, silica and silicates. In some cases, the mechanical properties of individual particles are of little or no concern. In other situations, density reduction might be a primary aim, as with the additions of hollow glass or ceramic microspheres. However, there are types of composite, notably for certain MMCs, in which particles of high stiffness and/or good resistance to fracture are needed. Chemical compatibility with the matrix is also relevant in many cases and there are likely to be optimal ranges of particle size, commonly of the order of a few microns or tens of microns. An example is provided by the incorporation of SiC grit, which has been in widespread commercial use for decades as an abrasive, into Al-based MMCs at levels around 20 vol%, with these materials often designed primarily for good wear resistance [23,24].

2.2 Statistics of Fibre Tensile Strength

2.2.1 Fracture of Brittle Materials

Most fibres are brittle. That is to say, they sustain little or no plastic deformation or damage up to the point when they fracture. Put another way, cracks can propagate with very little energy absorption. The *fracture energy* (or *critical strain energy release rate*, G_c) of glass is very low – not much more than the minimum for any material (i.e. 2γ , where γ is the surface energy), and with a typical value of around 10 J m^{-2} . It differs little for the various forms in which glass is manufactured. The tensile strength of a particular component made of such material is wholly dependent on the size (and orientation) of the largest flaw that is present, which is commonly somewhere on the free surface. The relationship between the size, c , of a surface flaw (oriented normal to the stress axis) and the tensile strength, σ_* , for a brittle material, is provided by the well-known *Griffith equation* – see Section 9.1.1, which can be expressed as

$$\sigma_* = \sqrt{\left(\frac{G_c E}{\pi c}\right)} \quad (2.1)$$

where E is the Young's modulus ($\sim 75 \text{ GPa}$ for glass). It follows that the strength is around 500 MPa when a $1 \text{ }\mu\text{m}$ flaw is present and 1.5 GPa for a $0.1 \text{ }\mu\text{m}$ flaw. On the other hand, a piece of glass with a scratch in it, which could easily have a depth of $100 \text{ }\mu\text{m}$ or more, will break under a moderate stress of a few tens of megapascal. In fact, freshly drawn glass fibres, with a diameter of the order of $10 \text{ }\mu\text{m}$, commonly have no flaw above a few tens of nanometres in size and so can have strengths of several GPa.

However, flaws above this size are readily introduced and it is clear that quoting a well-defined tensile strength is potentially misleading. In fact, a population of flaws is expected along the length of a fibre, so significant variations in strength are expected.

2.2.2 Weibull Analysis

This situation can be treated on a statistical basis. The approach, pioneered by Weibull in 1939, involves conceptually dividing a length L of fibre into a number of incremental lengths, $\Delta L_1, \Delta L_2$ etc. When a stress σ is applied, the parameter n_σ defines the number of flaws per unit length sufficient to cause failure under this stress. The fibre fractures when it has at least one incremental element with such a flaw and for this reason the analysis is often known as a *weakest link theory* (WLT). The probability of any given element failing depends on n_σ and on the length of the element. For the first element

$$P_{f1} = n_\sigma \Delta L_1 \quad (2.2)$$

The probability of the entire fibre surviving under this stress is the product of the probabilities of survival of each of the N individual elements that make up the fibre

$$P_S = (1 - P_{f1})(1 - P_{f2}) \dots (1 - P_{fN}) \quad (2.3)$$

Since the length of the elements can be taken as vanishingly small, the corresponding P_f values must be small. Using the approximation $(1-x) \approx \exp(-x)$, applicable when $x \ll 1$, leads to

$$P_S = \exp [-(P_{f1} + P_{f2} \dots + P_{fN})] \quad (2.4)$$

Substituting from Eqn (2.2), and the corresponding equations for the other elements

$$P_S = \exp [-Ln_\sigma] \quad (2.5)$$

An expression for n_σ is required if this treatment is to be of any use. Weibull proposed that most experimental data for failure of brittle materials conforms to an equation of the form

$$n_\sigma L_0 = \left(\frac{\sigma}{\sigma_0} \right)^m \quad (2.6)$$

in which m is usually termed the *Weibull modulus* and σ_0 is a normalising strength, which may for our purposes be taken as the most probable strength expected from a fibre of length L_0 . Making this assumption, the probability of failure of a fibre of length L , for an applied stress σ , is

$$P_f = 1 - \exp \left[- \left(\frac{L}{L_0} \right) \left(\frac{\sigma}{\sigma_0} \right)^m \right] \quad (2.7)$$

The Weibull modulus is an important parameter for characterising the strength distribution exhibited by the fibre (or any other brittle material). If the value of m is large (say >20), then it can be seen from Eqn (2.6) that stresses even slightly below the

normalising value σ_0 would lead to a low probability of failure, while if they were slightly above then a high probability would be predicted. Conversely, a low Weibull modulus (say, <5) would introduce much more uncertainty about the strength of a fibre. In practice, many ceramic materials exhibit Weibull moduli in the range 2–10, representing considerable uncertainty about the stress level at which any given specimen is likely to fail.

To check whether a set of strength values conforms to Eqn (2.7), it is convenient to rearrange the equation into a form in which a linear relationship is predicted. This is usually obtained via the logarithm of the probability of survival ($P_S = 1 - P_F$)

$$\ln(P_S) = -\left(\frac{L}{L_0}\right)\left(\frac{\sigma}{\sigma_0}\right)^m \quad (2.8)$$

so that

$$\ln\left(\frac{1}{P_S}\right) = \left(\frac{L}{L_0}\right)\left(\frac{\sigma}{\sigma_0}\right)^m \quad (2.9)$$

Taking logs again then gives

$$\ln\left(\ln\left(\frac{1}{P_S}\right)\right) = \ln(L) - \ln(L_0) + m \ln(\sigma) - m \ln(\sigma_0) \quad (2.10)$$

A plot, in this form, of data for P_S as a function of σ , should give a straight line with a gradient of m . An example is shown in Fig. 2.4, which gives data [25] for the strength distributions of three types of SiC monofilament. It can be seen that these data do

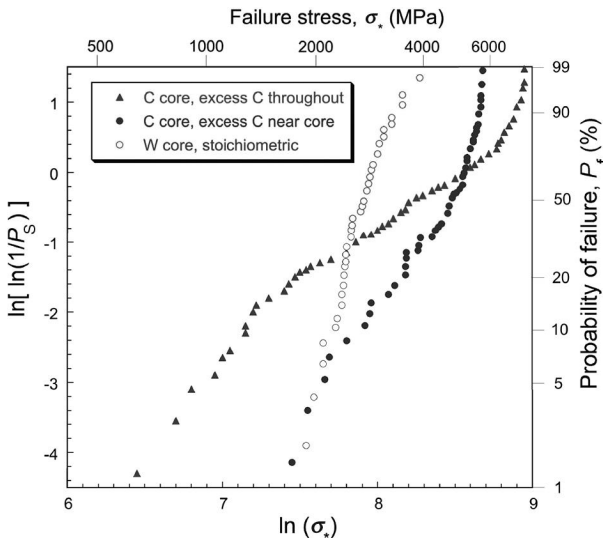


Fig. 2.4 Weibull plot [25] of failure strength data from three types of SiC monofilament, each manufactured under different conditions. These data were obtained by testing a large number of individual fibres of each type. The gradients (Weibull moduli, m) of the three plots are about 2, 4 and 8.

conform approximately to Eqn (2.10), in that the plots are more or less linear. The two carbon-cored fibres have about the same average strength, but rather different variabilities (m values of 2 and 4). The tungsten-cored fibre, on the other hand, has a lower average strength, but much lower variability ($m = 8$). These differences can be attributed to the nature and distribution of the flaws that are present.

The variability of strength exhibited by most ceramic fibres has important consequences for the mechanical behaviour of composite materials. It means, for example, that points of fibre fracture are often fairly randomly distributed and do not necessarily become concentrated in a single crack plane that propagates through the material. This leads to wide distributions of damage and promotes fibre pull-out (see Section 8.2), enhancing the toughness.

2.3 Matrices

The properties exhibited by various types of matrix are presented in Table 2.2. Information of this type, when considered together with data for reinforcements, allows potential systems to be appraised. For example, glass is evidently of no use for reinforcement of metals if enhancement of stiffness is a primary aim. Slightly more subtle points, such as whether fibre and matrix have widely differing thermal expansion coefficients (and would hence be prone to differential thermal contraction stresses), may also be explored. In practice, however, ease of manufacture (see Chapter 15) often assumes considerable importance. In the following sections some points are made concerning the factors that affect the choice of matrix.

2.3.1 Thermosetting Resins

The most commonly used resins are epoxy, unsaturated polyester and vinyl esters, which cover a very broad class of chemicals and a wide range of physical and mechanical properties. In thermosetting polymers, the liquid resin is converted into

Table 2.2 Overview of properties of several different types of matrix.

Matrix	Density ρ (kg m ⁻³)	Young's modulus E (GPa)	Shear modulus G (GPa)	Poisson ratio ν	Tensile strength σ_* (GPa)	Thermal expansivity α ($\mu\epsilon$ K ⁻¹)
Epoxy	1250	3.5	1.27	0.38	0.04	58
Polyester	1380	3.0	1.1	0.37	0.04	150
Polyether ether ketone (PEEK)	1300	4	1.4	0.37	0.07	45
Polycarbonate	1150	2.4	0.9	0.33	0.06	70
Polyurethane rubber	1200	0.01	0.003	0.46	0.02	200
Aluminium	2710	70	26	0.33	0.1–0.3	24
Magnesium	1740	45	7.5	0.33	0.1–0.2	26
Titanium	4510	115	44	0.33	0.4–1.0	10
Borosilicate glass	2230	64	28	0.21	0.05	3.2

a hard, rigid solid by chemical cross-linking, leading to formation of a tightly bound 3D network. This is usually done while the composite is being formed. The mechanical properties depend on the molecular units making up the network and on the length and density of the cross-links. The former depends on the chemicals used and the latter on the cross-links formed during curing. This can be done at room temperature, but it is usual to use a cure schedule that involves heating at one or more temperatures for predetermined times, to achieve optimum cross-linking and hence optimum properties. A relatively high-temperature final post-cure treatment is often given to minimise any changes in properties during service. Shrinkage during curing, and thermal contraction on cooling after curing, can lead to residual stresses in the composite – see Chapter 10.

It can be seen from the data in Table 2.2 that thermosets have slightly different properties from thermoplastics. Notable among these are much lower strains to failure. Thermosets are brittle, while thermoplastics can undergo appreciable plastic deformation. However, there are also significant differences between different types of thermoset. For example, epoxies are in general tougher than unsaturated polyesters or vinyl esters. In fact, epoxies are superior in most respects to alternative thermosetting systems, which are sometimes preferred simply on the grounds of lower cost.

2.3.2 Thermoplastics

Unlike thermosetting resins, thermoplastics are not cross-linked. They derive their strength and stiffness from inherent properties of the monomer units and high molecular weight. In glassy thermoplastics, such as poly(methyl methacrylate) (PMMA), there is a high concentration of molecular entanglements, which act like cross-links. Heating of amorphous materials above the *glass transition temperature*, T_g , creates molecular mobility, allowing these entanglements to unravel, so the material changes from a rigid solid to a viscous liquid. In crystalline polymers, heating leads to melting of the crystals (at T_m). Many thermoplastics are semi-crystalline, with $T_g < T_m$, and, for some of these, such as polyethylene, room temperature is above T_g , but below T_m . Such materials tend to be soft, and less brittle than fully glassy materials (which must operate below T_g). All of these polymers may have anisotropic structure and properties, depending on processing conditions. In amorphous regions, molecular alignment can be created by shear stresses arising during moulding or subsequent plastic deformation, while crystallographic texture (non-random crystallite orientation distributions) can arise from features of crystal nucleation and growth, or again from imposed plastic deformation, causing crystals to become reoriented.

Thermoplastics tend to exhibit good resistance to attack by chemicals and generally good thermal stability, particularly for certain advanced thermoplastics used in composites. Polyether ether ketone (PEEK), a semi-crystalline polymer, is a good example. The stiffness and strength of PEEK is little affected by heating up to 150°C, a temperature at which most polymers have become substantially degraded. Composites such as PEEK–60% carbon fibre are widely used in the aerospace industry. Other high-performance thermoplastics include polysulphones, polysulphides and polyimides.

Most of these are amorphous polymers. Many thermoplastics also show good resistance to absorption of water. All thermoplastics yield and undergo large deformations before final fracture and their mechanical properties are strongly dependent on temperature and strain rate. Another important feature of all thermoplastics is that under constant load conditions the strain tends to increase with time – i.e. creep occurs. This means that there may be a redistribution of the load between matrix and fibres during deformation and under in-service loading conditions.

One of the most significant features of thermoplastic composites is that processing tends to be more difficult than with thermosets. This is essentially because they are already polymeric, and hence highly viscous even when liquid, before the composite is fabricated. Although T_g and T_m are in many cases quite low, the melts they produce have high viscosities and cannot easily be impregnated into fine arrays of fibres. Usually it is necessary to ensure that flow distances are short, for example by interleaving thin polymer sheets with fibre preforms, and to apply substantial pressures for appreciable times (see Section 15.1). Once fibre and matrix have been brought together in some way, then various shaping operations, such as injection moulding, can be carried out.

2.3.3 Metal Matrices

The development of metal matrix composites has largely been concentrated on three metals: aluminium, magnesium and titanium. Metals are normally alloyed with other elements to improve their physical and mechanical properties, and a wide range of alloy compositions is available. Final properties are strongly influenced by thermal and mechanical treatments, which determine the microstructure. Some typical properties of common metal matrices are given in Table 2.2. The metals used for composites are usually ductile and essentially isotropic. Unlike polymers, the increases in stiffness achieved by incorporation of the reinforcement are often relatively small. However, important improvements are often achieved in properties such as wear characteristics, creep performance and resistance to thermal distortion. All three metals are very reactive, with a strong affinity for oxygen. This has implications for the production of composites, particularly in regard to chemical reactions at the interface between the matrix and the reinforcement, which has proved especially troublesome for titanium.

2.3.4 Ceramic Matrices

Four main classes of ceramic have been used for ceramic matrix composites. *Glass ceramics* are complex glass-forming oxides, such as boro-silicates and aluminosilicates, which have been heat treated so that a crystalline phase precipitates to form a fine dispersion in the glassy phase. Glass ceramics have lower softening temperatures than crystalline ceramics and are easier to fabricate – this is an especially important consideration for ceramic composites. *Engineering ceramics*, such as SiC, Si₃N₄, Al₂O₃ and ZrO₂, are fully crystalline and have the normal structure of crystalline grains randomly oriented relative to each other. There has been considerable interest in

reinforcement of *cement* and *concrete*, usually adding short fibres in such a way that moulding capabilities are not severely impaired. Finally, carbon–carbon composites, produced by vapour infiltration of an array of carbon fibres, form a specialised, but commercially important, subclass of composite material. They find use not only in the long-standing application of aircraft brakes, but also in various other components in the aerospace industry with demanding requirements [26].

The objective of adding reinforcement to ceramics is usually to improve their toughness. Ceramics are very brittle and even a small increase in toughness may be worthwhile. When ceramics are added, the toughness increase often comes from repeated crack deflection at interfaces, in which case the nature of the interface assumes overriding importance [27]. However, it should be noted that substantial toughness enhancement can often be achieved by introducing metallic reinforcement, particularly in the form of fibres. This may reduce the high-temperature performance of the material, although some metal fibres, such as certain stainless steels, have very good stability at elevated temperatures. Systems such as alumina reinforced with ~15 vol% of stainless steel fibres can offer attractive combinations of toughness and potential for usage at high temperatures [28,29], and their usage is likely to increase in the future.

2.4 Long Fibre Composite Architectures

2.4.1 Laminates

In many situations, a relatively high value of the fibre volume fraction, f , is desirable. The easiest way to achieve this is to align (long) fibres in a given direction. In principle, an assembly of close-packed cylinders can occupy over 90% of the volume. In practice, this is not achievable, partly because it would require many of the fibres to be in contact with their neighbours, creating several problems. However, values of around 60–70% are realistic, consistent with the need to keep fibres apart and with manufacturing constraints. Furthermore, for many applications, while good properties (primarily stiffness and strength) are commonly required in various directions within a sheet or plate, properties normal to this plane (i.e. in the through-thickness direction) are usually much less important (because the component is unlikely to be loaded in that direction). The basic building block for composite structures is thus often a thin sheet containing fibres aligned in one direction, termed a *lamina* or *ply*.

In order to achieve suitable properties in various directions within the plane (often tailored to the expected loading of the component during service) *laminae* are stacked in a predetermined sequence to create a *laminate*. For the prediction of elastic properties of the component as a whole, each lamina may be regarded as homogeneous in the sense that the fibre distribution and volume fraction are uniform throughout. The properties of the laminate can thus be predicted for any given *stacking sequence* – see Chapter 4. A sequence is shown in Fig. 2.5, with an indication of the nomenclature used to describe it.

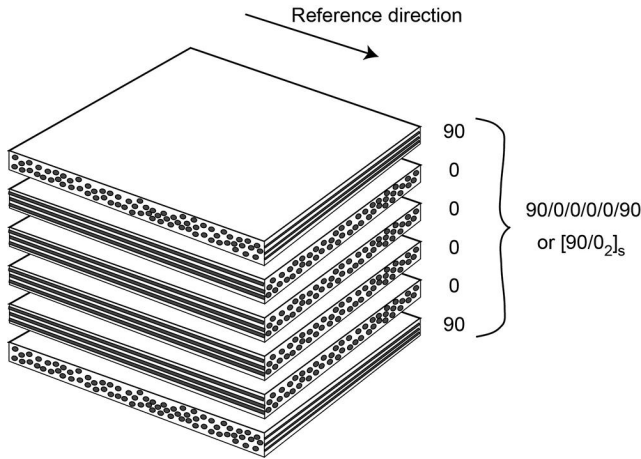


Fig. 2.5 Schematic depiction of a fibre laminate (stack of plies), illustrating the nomenclature system.

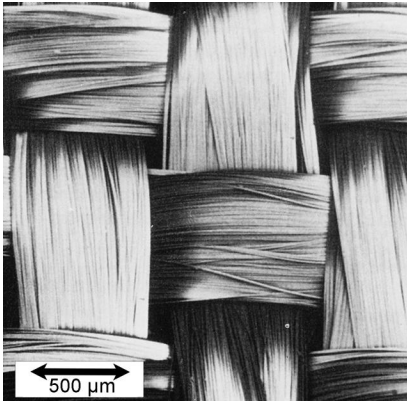


Fig. 2.6 SEM micrograph of a woven roving assembly of long glass fibres.

2.4.2 Woven and Planar Random Fibre Assemblies

Continuous fibres can be assembled in ways other than stacking of unidirectional plies. Much of this is done using technology originally developed for textile processes – i.e. *weaving*, *braiding* and *knitting*. The arrangement of fibres in a typical woven assembly is shown in Fig. 2.6. In this case, the angle between the warp and weft directions is 90° . The flexibility of this type of fibre assembly allows draping and shaping to occur, facilitating use in non-planar structures. The angle between the warp and weft directions will affect these characteristics. Of course, this type of structure leads to a rather inhomogeneous distribution of the fibres. Furthermore, a high fibre content is not possible – the maximum volume fraction is usually not much more than about 20–25%. Therefore, while use of this type of starting material is convenient in terms

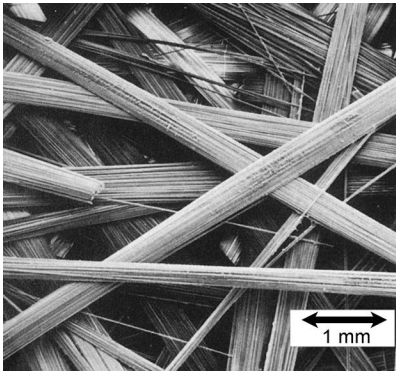


Fig. 2.7 SEM micrograph of a chopped strand mat glass fibre preform.

of handling and processing, it is not normally used for very demanding applications. Nevertheless, usage is quite extensive.

A commonly used form of fibre distribution, particularly for low-cost applications, is *chopped strand mat*. Bundles of relatively long fibres are assembled together with random in-plane orientations, as shown in Fig. 2.7. These are created by sedimentation of fibre bundles from suspension in a fluid. The material is easy to handle as a preform and the resultant composite material has isotropic in-plane properties. However, the fibre volume fraction is limited to relatively low values ($< \sim 20\%$). Moreover, the scope for tailoring of the properties in different in-plane directions, which is considerable for laminates and exists to a limited degree with woven assemblies, is not available for this type of material.

2.5 Short Fibre Configurations

While most high-performance composites tend to be based on long (continuous) fibres, there are many applications in which, for various reasons, short fibres, or even particles, are preferred. This tends to allow more versatility in the processing, so that, for example, the composite material itself can be subjected to forming processes such as extrusion, drawing, rolling, etc. These processes are, of course, widely used for metals, but cannot normally be applied to long fibre composites. Characterisation of the fibre architecture is more complex for short fibre composites, since they may not be aligned within a plane and there is more likelihood of them displaying large local variations in orientation. Moreover, while clustering (local variations in position) may be an issue for long fibres, such effects are commonly more pronounced with short fibres (and particles).

2.5.1 Fibre Orientation Distributions

There are several ways of both measuring and characterising fibre orientation distributions. Some involve examining polished sections, although these are rather

time-consuming and outdated. The most powerful technique, now in widespread use, is that of computed tomography, which involves analysis of absorption images obtained by passing an X-ray beam through a sample in different directions. Associated software commonly allows the resultant fibre architecture, which can be visualised in 3D, to be transferred directly into numerical (FEM) models, where it can be meshed and used to predict various characteristics.

Orientation distributions in 3D are commonly represented on a *stereographic projection* (stereogram). Thus, *texture* information for polycrystals can be presented as *pole figures*, which depict the relative frequencies of the orientation of specified crystallographic directions, relative to the external frame of reference. There are in fact several issues and possible options when obtaining and presenting such information [30]. Representation of fibre distributions is simpler than for the texture of polycrystals, since only the orientation of the fibre axis is required and each fibre is represented as a point on the stereogram. In fact, a random (isotropic) 3D distribution of orientations does not plot as a uniform density of points; the points are clustered near the centre and are sparse towards the edges. This is illustrated in Fig. 2.8, which shows (a) how two directions, 1 and 2, plot as P_1 and P_2 on the projection and (b) how an isotropic

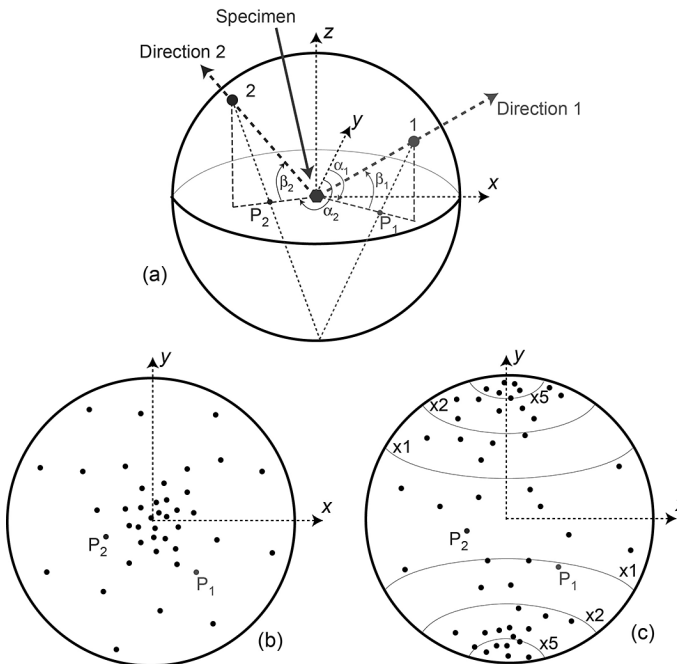


Fig. 2.8 Representation of orientation distributions in 3D, using the stereographic projection. (a) Construction of the stereogram, showing how two directions, 1 and 2, are plotted as points P_1 and P_2 where the lines from 1 and 2 to the 'south pole' intersect the 'equatorial plane'. (b) Stereogram of a set of randomly oriented directions. (c) Stereogram of a set of directions, with a systematic bias towards the reference direction y, with superimposed contours separating regions in which the population densities are different multiples of the random case.

distribution of directions plots as a non-uniform density of points. The most effective way to present fibre distribution information is in the form of a series of contours, representing the ratio of the local density of points to that expected for an isotropic distribution. Such contours, which are normally constructed using a computer program, are shown in Fig. 2.8(c). This allows the strength of any preferred orientation to be characterised by a single figure, since the value of the highest contour present can readily be established.

An example [31] of the application of such procedures to a fibre orientation distribution is presented in Fig. 12.5 for the case of a metallic fibre network material – i.e. a ‘composite’ for which the ‘matrix’ is air. (Such highly porous materials are covered in Chapter 12.) Of course, this case has the advantage of very high ‘contrast’ (difference between the X-ray absorption rates of fibre and matrix), although in practice it is usually adequate for most composite systems. Visualisations are shown in Fig. 12.5 for two different fibre network materials, both made by sintering assemblies of (relatively coarse) stainless steel fibres, (a) without and (b) with a compression procedure that created a non-random distribution of the orientation of individual fibre segments (between joints). Also shown are corresponding extracted fibre orientation distribution data for the two materials, taken from the two stereograms. It can be seen that compression has created a marked tendency for the fibres to lie at relatively large angles to the unique (pressing) direction, while the uncompressed sample was approximately isotropic. This is clearly as expected, although the strength of the effect will depend on fibre segment length, and perhaps also on fibre yielding and work hardening characteristics, as well as on the compression pressure.

It may also be noted that, under certain circumstances, variations in local fibre orientation can have a significant effect on certain properties for long fibre composites, despite the fact that these variations tend to be relatively small. An example is provided by the axial compressive strength of uniaxial composites (‘struts’), which is sensitive to fibre ‘waviness’ along the length of the component – see Section 8.1.3.

2.5.2 Clustering of Fibres and Particles

Examination of laminae and laminate cross-sections usually reveals that the positional distribution of the fibres is not entirely uniform and this tendency is often considerably more marked with short fibres and particles. This is unlikely to have much influence on most ‘macroscopic’ properties, such as stiffness, thermal expansivity and thermal conductivity. However, it could be relevant to the onset of damage and failure, since local inhomogeneities can influence both the initiation and propagation of cracks and might also be relevant to localised plasticity. There are therefore certain circumstances in which it can be helpful to characterise the severity of clustering (which is likely to be affected by the details of the processing route).

An example of this is provided by the plot [32] shown in Fig. 2.9, which confirms that a clear correlation could be established between the ductility of a particular type of MMC (an Al-9Si-0.5Mg alloy containing 20 vol% of SiC particulate, with average size ~12 μm) and the severity of the clustering of these particles. Different variants of this

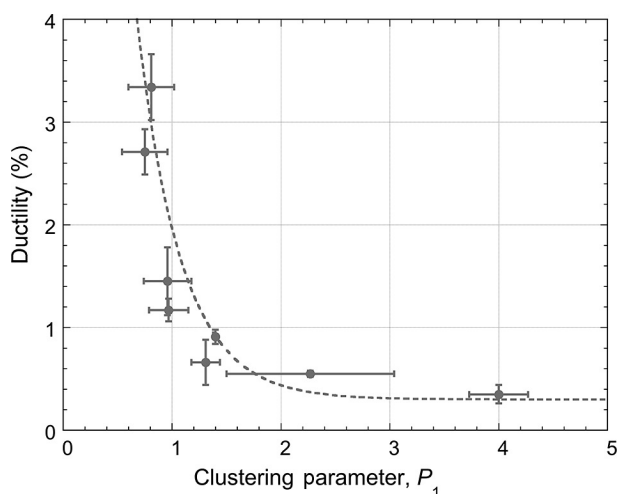


Fig. 2.9 Measured ductility of various composite materials, all based on an Al alloy matrix containing 20 vol% of SiC particulate, as a function of a parameter characterising the severity of clustering of the particles in the microstructure. This varied as a result of changes in the casting and thermo-mechanical processing procedures employed during production [32].

material were produced by altering the processing procedures and conditions, ensuring in each case that there was no porosity present – all samples were subjected before testing to a hot isostatic pressing operation – and that the matrix microstructure was essentially the same in all cases. The clustering parameter was obtained via analysis of a series of metallographic sections, with the locations of particle centres being established and a Dirichlet tessellation procedure then being used to characterise their distribution. The clustering severity parameter used in the plot was the ratio of the variance of the distribution of cell areas to that for a random distribution with the same average areal density of particles. Of course, this is a limited analysis, being confined, for example, to 2D examination, but it does at least confirm that clustering can be an issue (in tending to promote cracking, at least in this type of composite).

References

1. Bennett, SC and DJ Johnson, Structural heterogeneity in carbon fibres, in *Proc. 5th London Carbon and Graphite Conference*. Society for the Chemical Industry, 1978, pp. 377–386.
2. Tanaka, F and T Okabe, Historical review of processing, microstructures, and mechanical properties of PAN-based carbon fibers, in *Comprehensive Composite Materials II*, Gdoutos, EE, editor. Elsevier, 2018, pp. 66–85.
3. Yusof, N and AF Ismail, Post spinning and pyrolysis processes of polyacrylonitrile (PAN)-based carbon fiber and activated carbon fiber: a review. *Journal of Analytical and Applied Pyrolysis* 2012; **93**: 1–13.
4. Huang, XS, Fabrication and properties of carbon fibers. *Materials* 2009; **2**(4): 2369–2403.

5. Bermudez, V, S Lukubira and AA Ogale, Pitch precursor-based carbon fibers, in *Comprehensive Composite Materials II*, Gdoutos, EE, editor. Elsevier, 2018, pp. 41–65.
6. DiBenedetto, AT, Tailoring of interfaces in glass fiber reinforced polymer composites: a review. *Materials Science and Engineering A: Structural Materials, Properties, Microstructure and Processing* 2001; **302**(1): 74–82.
7. Li, H, T Charpentier, JC Du and S Vennam, Composite reinforcement: recent development of continuous glass fibers. *International Journal of Applied Glass Science* 2017; **8**(1): 23–36.
8. Dwight, DW and S Begum, Glass fiber reinforcements, in *Comprehensive Composite Materials II*, Gdoutos, EE, editor. Elsevier, 2018, pp. 243–268.
9. Singh, TJ and S Samanta, Characterization of Kevlar fiber and its composites: a review. *Materials Today: Proceedings* 2015; **2**(4–5): 1381–1387.
10. Yang, HM, Glass fiber reinforcements, in *Comprehensive Composite Materials II*, Gdoutos, EE, editor. Elsevier, 2018, pp. 187–217.
11. Medina, LA and J Dzalto, Natural fibers, in *Comprehensive Composite Materials II*, Gdoutos, EE, editor. Elsevier, 2018, pp. 269–294.
12. Wawner, FE, Boron and silicon carbide fibers (CVD), in *Comprehensive Composite Materials II*, Gdoutos, EE, editor. Elsevier, 2018, pp. 167–186.
13. Moongkhamklang, P, VS Deshpande and HNG Wadley, The compressive and shear response of titanium matrix composite lattice structures. *Acta Materialia* 2010; **58**(8): 2822–2835.
14. Zhao, DF, HZ Wang and XD Li, Development of polymer-derived SiC fiber. *Journal of Inorganic Materials* 2009; **24**(6): 1097–1104.
15. Ichikawa, H and T Ishikawa, Silicon carbide fibers (organometallic pyrolysis), in *Comprehensive Composite Materials II*, Gdoutos, EE, editor. Elsevier, 2018, pp. 127–166.
16. Berger, MH and AR Bunsell, Oxide fibers, in *Comprehensive Composite Materials II*, Gdoutos, EE, editor. Elsevier, 2018, pp. 218–242.
17. Dhingra, AK, Alumina Fiber FP. *Philosophical Transactions of the Royal Society A: Mathematical Physical and Engineering Sciences* 1980; **294**(1411): 411–417.
18. Seeger, T, P Kohler-Redlich and M Ruhle, Synthesis of nanometer-sized SiC whiskers in the arc-discharge. *Advanced Materials* 2000; **12**(4): 279–282.
19. Silva, PC and JL Figueiredo, Production of SiC and Si₃N₄ whiskers in C+SiO₂ solid mixtures. *Materials Chemistry and Physics* 2001; **72**(3): 326–331.
20. Li, J, T Shirai and M Fuji, Rapid carbothermal synthesis of nanostructured silicon carbide particles and whiskers from rice husk by microwave heating method. *Advanced Powder Technology* 2013; **24**(5): 838–843.
21. Zhang, Q, JQ Huang, WZ Qian, YY Zhang and F Wei, The road for nanomaterials industry: a review of carbon nanotube production, post-treatment, and bulk applications for composites and energy storage. *Small* 2013; **9**(8): 1237–1265.
22. Lu, W, Q Li and TW Chou, Carbon nanotube based fibers, in *Comprehensive Composite Materials II*, Gdoutos, EE, editor. Elsevier, 2018, pp. 13–40.
23. Deuis, RL, C Subramanian and JM Yellup, Abrasive wear of aluminium composites: a review. *Wear* 1996; **201**(1–2): 132–144.
24. Alpas, AT, S Bhattacharya and IM Hutchings, Wear of particulate metal matrix composites, in *Comprehensive Composite Materials II*, Clyne, TW, editor. Elsevier, 2018, pp. 137–172.
25. Martineau, P, M Lahaye, R Pailler, R Naslain, IM Couzi and F Cruege, SiC filament/titanium matrix composites regarded as model composites. Part 1: filament microanalysis and strength characterization. *Journal of Materials Science* 1984; **19**: 2731–2748.

26. Taylor, RL, SBV Siva and PSR Sreekanth, Carbon matrix composites, in *Comprehensive Composite Materials II*, Ruggles-Wrenn, MB, editor. Elsevier, 2018, pp. 339–378.
27. Krenkel, W and F Reichert, Design objectives and design philosophies, interphases and interfaces in fiber-reinforced CMCs, in *Comprehensive Composite Materials II*, Ruggles-Wrenn, MB, editor. Elsevier, 2018, p. 1–18.
28. Pemberton, SR, EK Oberg, J Dean, D Tsarouchas, AE Markaki, L Marston and TW Clyne, The fracture energy of metal fibre reinforced ceramic composites (MFCs). *Composites Science and Technology* 2011; **71**(3): 266–275.
29. Clyne, TW and LW Marston, Metal fibre-reinforced ceramic composites and their industrial usage, in *Comprehensive Composite Materials II*, Clyne, T W, editor. Elsevier, 2018, pp. 464–481.
30. Callahan, PG, M Echlin, TM Pollock, S Singh and M De Graef, Three-dimensional texture visualization approaches: theoretical analysis and examples. *Journal of Applied Crystallography* 2017; **50**: 430–440.
31. Tan, JC, JA Elliott and TW Clyne, Analysis of tomography images of bonded fibre networks to measure distributions of fibre segment length and fibre orientation. *Advanced Engineering Materials* 2006; **8**(6): 495–500.
32. Murphy, AM, SJ Howard and TW Clyne, Characterisation of the severity of particle clustering and its effect on the fracture of particulate MMCs. *Materials Science and Technology* 1998; **14**: 959–968.

3 Elastic Deformation of Long Fibre Composites

In the previous chapter, some background was provided about types of reinforcement and their distribution within different matrices. Attention is now turned to predicting the behaviour of the resulting composites. The prime concern is with mechanical properties. The reinforcement is usually designed to enhance the stiffness and strength of the matrix. The details of this enhancement can be rather complex. The simplest starting point is the elastic behaviour of a composite with aligned long (continuous) fibres. This arrangement creates high stiffness (and strength) in the fibre direction. However, it is also important to understand the behaviour when loaded in other directions, so the treatment also covers transverse loading. In this chapter, and in the following one, perfect bonding is assumed at the fibre/matrix interface. Details concerning this region, and consequences of imperfect bonding, are considered in Chapter 6.

3.1 Axial Young's Modulus

The simplest treatment of the elastic behaviour of aligned long fibre composites is based on the premise that the material can be treated as if it were composed of parallel slabs of the two constituents bonded together, with relative thicknesses in proportion to the volume fractions of matrix and fibre. This is illustrated in Fig. 3.1, which compares the assumptions imposed by use of the 'slab model' with the situation in an actual long fibre composite under different types of applied load. The two slabs are constrained to have the same lengths parallel to the bonded interface. Thus, if a stress is applied in the direction of fibre alignment (termed the 1 direction throughout this book), then both constituents experience the same strain in this direction, ε_1 . This 'equal strain' condition is valid for loading along the fibre axis, provided there is no interfacial sliding.

It is now a simple matter to derive an expression for the Young's modulus of the composite, E_1 . The axial strain in the fibre and the matrix must correspond to the ratio between the stress and the Young's modulus for each of the two components, so that

$$\varepsilon_1 = \varepsilon_{1f} = \frac{\sigma_{1f}}{E_f} = \varepsilon_{1m} = \frac{\sigma_{1m}}{E_m} \quad (3.1)$$

Hence, for a composite in which the fibres are much stiffer than the matrix ($E_f \gg E_m$), the reinforcement bears a much higher stress than the matrix ($\sigma_{1f} \gg \sigma_{1m}$) and there is a

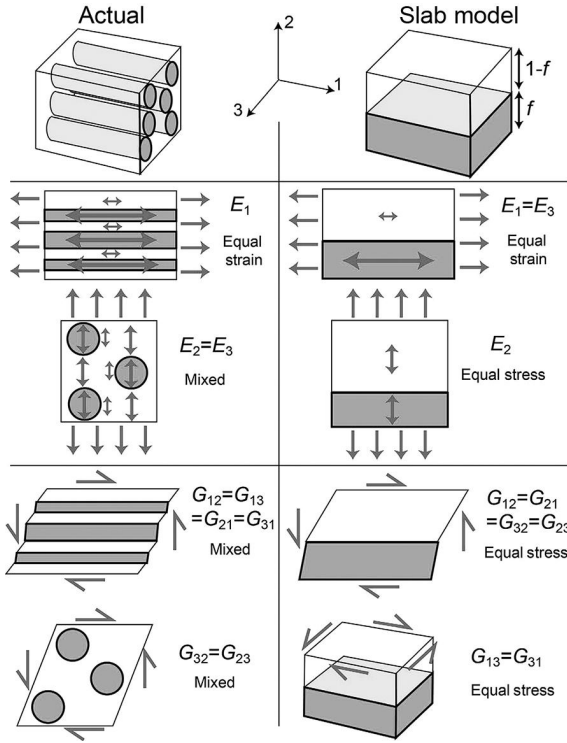


Fig. 3.1 Schematic illustration of loading geometry and distributions of stress and strain, and effects on the Young's moduli and shear moduli, for a uniaxial fibre composite and for the slab model representation.

redistribution of the load. The overall composite stress σ_1 can be expressed in terms of the two contributions being made to the load

$$\sigma_1 = (1 - f)\sigma_{1m} + f\sigma_{1f} \quad (3.2)$$

The Young's modulus of the composite can now be written as

$$E_1 = \frac{\sigma_1}{\varepsilon_1} = \frac{(1 - f)\sigma_{1m} + f\sigma_{1f}}{\sigma_{1f}/E_f} = E_f \left[\frac{(1 - f)\sigma_{1m}}{\sigma_{1f}} + f \right]$$

Using the ratio between the stress in the two constituents given by Eqn (3.1), this simplifies to

$$E_1 = (1 - f)E_m + fE_f \quad (3.3)$$

This well-known *rule of mixtures* indicates that the composite stiffness is simply a weighted mean between the moduli of the two components, depending only on the volume fraction of fibres. It is expected to be valid to a high degree of precision, providing the fibres are long enough for the equal strain assumption to apply. (The details of this condition are examined in Chapter 5.) Very minor deviations from the

equation are expected as a result of effects that arise when the Poisson ratios of the two constituents are not equal. More advanced treatments (such as the Eshelby model described in Chapter 5) show that the predicted discrepancies are extremely small in all cases. The rule of mixtures can readily be confirmed experimentally for uniaxial long fibre composites. The equal strain treatment is often described as a *Voigt model*.

3.2 Transverse Young's Modulus

Accurate prediction of the transverse stiffness is far more difficult than for the axial value. In addition, experimental measurement is more prone to error, partly as a result of higher stresses in the matrix – which can, for example, cause polymeric matrices to creep under modest applied loads. The simplest approach is to assume that the system can again be represented using the ‘slab model’ depicted in Fig. 3.1. In the fibre composite shown in the left side of Fig. 3.1, both 2 and 3 directions are transverse to the fibres. An obvious problem with the slab model is that the two transverse directions are not identical; direction 3 is equivalent to the axial direction (direction 1). In reality the matrix is subjected to an effective stress intermediate between the full applied stress operating on the matrix when it is normal to the plane of the slab interface and the reduced value calculated in Section 3.1 for loading parallel to this interface – i.e. a ‘mixed’ condition applies, as indicated in Fig. 3.1. Before considering this any further, the limiting case of the ‘equal stress’ model will be examined. When a stress is applied in the 2 direction

$$\sigma_2 = \sigma_{2f} = \varepsilon_{2f}E_f = \sigma_{2m} = \varepsilon_{2m}E_m \quad (3.4)$$

The overall net strain can be written in terms of the two contributions to it

$$\varepsilon_2 = f\varepsilon_{2f} + (1 - f)\varepsilon_{2m} \quad (3.5)$$

from which the composite modulus can be expressed as

$$E_2 = \frac{\sigma_2}{\varepsilon_2} = \frac{\sigma_{2f}}{f\varepsilon_{2f} + (1 - f)\varepsilon_{2m}}$$

Substituting expressions for ε_{2f} and ε_{2m} derived from Eqn (3.4) leads to

$$E_2 = \left[\frac{(1 - f)}{E_m} + \frac{f}{E_f} \right]^{-1} \quad (3.6)$$

This equal stress treatment, giving an ‘inverse rule of mixtures’, is often described as a ‘*Reuss model*’.

Although this treatment is simple and convenient, it gives a relatively poor approximation for E_2 . It is instructive to consider the true nature of the stress and strain distributions in a fibre composite during this type of loading, which is depicted schematically in Fig. 3.1 (next to the ‘ $E_2 = E_3$, Mixed’ label). Regions of the matrix ‘in series’ with the fibres (close to them and in line along the loading direction) are subjected to a high stress similar to that carried by the reinforcement, whereas regions

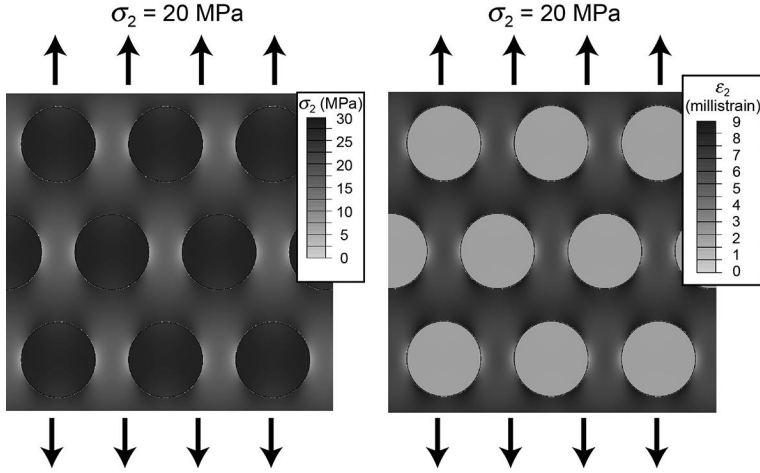


Fig. 3.2 Stress and strain fields in a transverse section of a polyester-40 vol% glass long fibre composite, with the fibres in a hexagonal array, subject to a transverse (vertical) stress of 20 MPa. The elastic properties used for fibre and matrix are those in Tables 2.1 and 2.2. (Courtesy of Dr M. Burley.)

‘in parallel’ with the fibres (adjacent laterally) are constrained to have the same (low) strain as the reinforcement and hence carry a low stress, as shown in the figure.

A degree of quantification of this picture is provided by Fig. 3.2, which shows stress and strain fields obtained using the finite element method (FEM). These relate to a long fibre composite under a transverse stress of 20 MPa. It may be noted that, while this is a moderate stress, the levels thus created at certain locations in the matrix (near to the interface) might be sufficient to cause cracking or debonding. It can also be seen that the distribution of matrix strain is very inhomogeneous, with the peak levels (approaching 1%) quite possibly being high enough to cause some kind of failure (at or near the interface). In practice, composite components are usually designed to ensure that transverse loads on unidirectionally reinforced material remain relatively low.

The non-uniform distribution of stress and strain during transverse loading means that the simple equal stress model is inadequate for many purposes. The slab model gives an underestimate of the Young’s modulus, which constitutes a lower bound. Various empirical or semi-empirical expressions designed to give more accurate estimates have been proposed. The most successful of these is that due to Halpin and Tsai [1]. This is not based on rigorous elasticity theory, but broadly takes account of enhanced fibre load-bearing, relative to the equal stress assumption. Their expression for the transverse stiffness is

$$E_2 = \frac{E_m(1 + \zeta\eta f)}{(1 - \eta f)}, \quad \text{in which } \eta = \frac{\left(\frac{E_f}{E_m} - 1\right)}{\left(\frac{E_f}{E_m} + \zeta\right)} \quad (3.7)$$

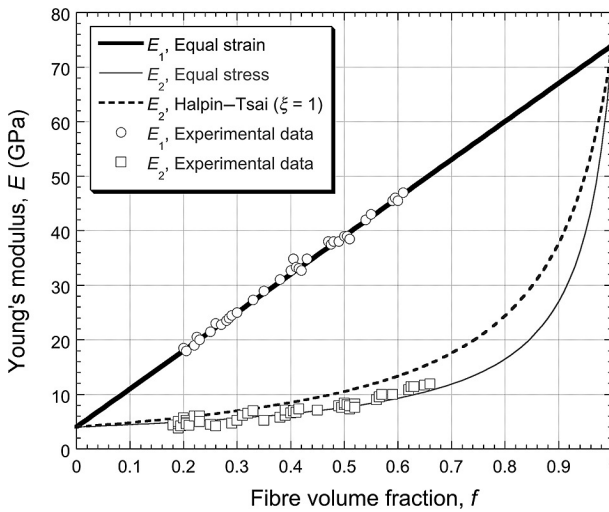


Fig. 3.3 Comparison between experimental data [2] for the axial and transverse Young's moduli, E_1 and E_2 , for polyester-glass fibre composites and corresponding predictions from the equal strain model (Eqn (3.3)) for E_1 and the equal stress (Eqn (3.6)) and Halpin-Tsai (Eqn (3.7)), with $\xi = 1$) models for E_2 . The experimental E_2 values have been affected by inelastic deformation of the matrix.

The value of ξ (xi) may be taken to be adjustable, but its magnitude is of the order of unity. The expression gives the correct values in the limits of $f = 0$ and $f = 1$ and in general gives good agreement with experiment over the complete range of fibre content.

A comparison is presented in Fig. 3.3 between the predictions of Eqns (3.3), (3.6) and (3.7) and experimental data for a glass fibre-polyester system. It is clear that the equal strain treatment (Eqn (3.3)) is in close agreement with data for the axial modulus. For the transverse modulus, the situation is less clear. Firstly, the experimental data show considerable scatter; some of the values actually lie below the equal stress prediction (Eqn (3.6)), which should constitute a lower bound. Secondly, many of the values appear to lie closer to the equal stress curve than to the Halpin-Tsai prediction, although this is less obvious for the high fibre contents. This behaviour is almost certainly the result of inelastic deformation of the matrix. These values were obtained by mechanical loading experiments in which relatively large stresses were present for appreciable times. (This is much less significant during axial loading, since the matrix stresses are so low.) Plastic deformation and creep may occur during a transverse test of this type, particularly with thermoplastic polymers, and this will lead to an underestimate of the true stiffness. In general, tests with stronger and more creep-resistant matrices, or under conditions where all the stresses are kept low and are of short duration (as with dynamic methods of stiffness measurement [3]), have confirmed that the transverse moduli of long fibre composites agree quite well with the Halpin-Tsai prediction (Eqn (3.7)).

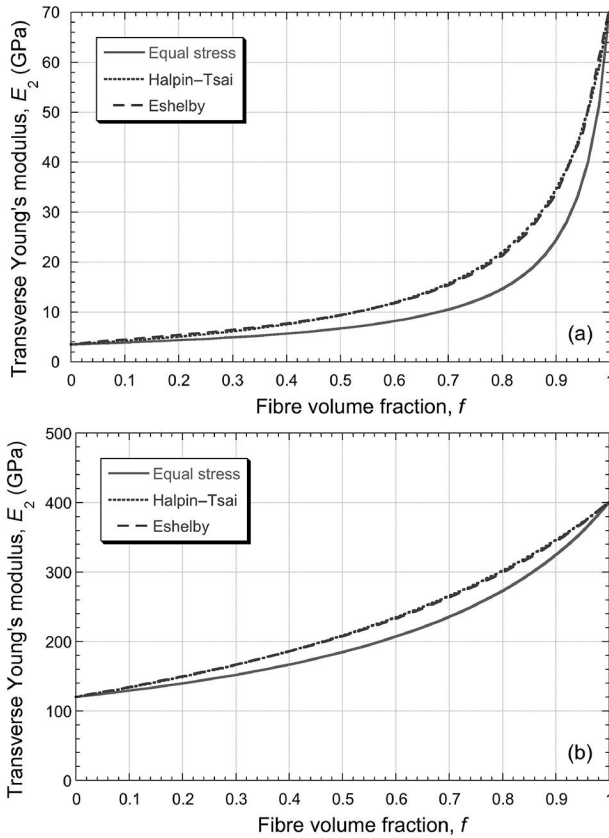


Fig. 3.4 Predicted dependence on fibre volume fraction of the transverse Young's moduli of continuous fibre composites, according to the equal stress (Eqn (3.6)), Halpin-Tsai, (Eqn (3.7)) and Eshelby models for (a) glass fibres in epoxy and (b) silicon carbide fibres in titanium.

Beyond these simple models for predicting the transverse modulus, there are powerful, but complex, analytical tools such as the Eshelby equivalent homogeneous inclusion approach (see Chapter 5) and of course numerical techniques such as finite element modelling (FEM), which is now ubiquitous in many areas of science and engineering. The plots shown in Fig. 3.4 give an idea of the errors likely to be introduced in real cases by use of the equal stress expression, as compared with the Eshelby method, which is expected to be much more reliable. It can be seen that Eqn (3.6) gives a significant underestimate for both polymer matrix composites (PMCs) and metallic matrix composites (MMCs), which respectively have large and small fibre/matrix modulus ratios. The Halpin-Tsai expression (Eqn (3.7)), on the other hand, is fairly accurate.

In practice, the behaviour may be influenced by other factors, which are difficult to incorporate into simple models. These include the effects of fibre misalignment, elastic anisotropy of the fibre (or of the matrix – e.g. for a textured polycrystalline metal) or the early onset of an inelastic response. Nevertheless, it should be noted that, even in the absence of any such complications, use of the equal stress model introduces significant

errors: this should be borne in mind, for example, if it is being used in laminate elasticity analysis (see Chapter 4).

3.3 Other Elastic Constants

3.3.1 Shear Moduli

The shear moduli of composites can be predicted in a similar way to the axial and transverse stiffnesses, using the slab model. This is done by evaluating the net shear strain induced when a shear stress is applied to the composite, in terms of the individual displacement contributions from the two constituents. It is important to understand the nomenclature convention that is used. A shear stress designated τ_{ij} ($i \neq j$) refers to a stress acting in the i direction on the plane with a normal in the j direction. Similarly, a shear strain γ_{ij} is a rotation towards the i direction of the j axis. The shear modulus G_{ij} is the ratio of τ_{ij} over γ_{ij} . Since the composite body is not rotating, the condition $\tau_{ij} = \tau_{ji}$ must hold. In addition, $G_{ij} = G_{ji}$, so that $\gamma_{ij} = \gamma_{ji}$. Also, the 2 and 3 directions are equivalent in an aligned fibre composite, so it follows that there are two shear moduli, with $G_{12} = G_{21} = G_{13} = G_{31} \neq G_{23} = G_{32}$.

There are also two shear moduli for the slab model (Fig. 3.1), but these are unlikely to correspond closely with the values for the fibre composite. The stresses τ_{12} and τ_{21} are assumed to operate equally within both of the constituents. The derivation is similar to the equal stress treatment leading to Eqn (3.6) for transverse stiffness

$$\tau_{12} = \tau_{12f} = \gamma_{12f} G_f = \tau_{12m} = \gamma_{12m} G_m$$

where γ_{12f} and γ_{12m} are the individual shear strains in the two constituents. The total shear strain is found by summing the two contributions to the total shear displacement in the 1 direction

$$\gamma_{12} = \frac{(u_{1f} + u_{1m})}{f + (1-f)} = f\gamma_{12f} + (1-f)\gamma_{12m}$$

$$\therefore G_{12} = \frac{\tau_{12}}{\gamma_{12}} = \frac{\tau_{12f}}{f\gamma_{12f} + (1-f)\gamma_{12m}} = \left[\frac{f}{G_f} + \frac{(1-f)\gamma_{12m}}{\tau_{12f}} \right]^{-1}$$

$$\text{i.e.} \quad G_{12} = \left[\frac{f}{G_f} + \frac{(1-f)}{G_m} \right]^{-1} \quad (3.8)$$

The other shear modulus shown by the slab model, $G_{13} = G_{31}$ in Fig. 3.1, corresponds to an equal shear strain condition and is analogous to the axial tensile modulus case. It is readily shown that

$$G_{13} = fG_f + (1-f)G_m \quad (3.9)$$

which is similar to Eqn (3.3). It may be noted that neither the equal stress condition nor the equal strain condition are close to the situation during shearing of the fibre composite, in which the strain partitions unevenly within the matrix. Therefore neither of the above equations is expected to be very reliable, particularly the equal strain expression.

It is not obvious just how poor the approximation represented by Eqn (3.8) is likely to be, nor even which of the two actual shear moduli it will approach more closely. In fact, more rigorous methods predict that the values of G_{12} and G_{23} are rather close to each other, with G_{12} slightly larger in magnitude. Eqn (3.8) gives a significant underestimate relative to both of them, while Eqn (3.9) is a gross overestimate. In view of this, the semi-empirical expressions of Halpin and Tsai [1], mentioned in the previous section, are frequently employed. In this case, the appropriate equation is:

$$G_{12} = \frac{G_m(1 + \xi\eta f)}{(1 - \eta f)}, \text{ in which } \eta = \frac{\left(\frac{G_f}{G_m} - 1\right)}{\left(\frac{G_f}{G_m} + \xi\right)} \quad (3.10)$$

and the parameter ξ is again often taken to have a value of around unity. This has been done for the curves in Fig. 3.5, which shows comparisons between the predictions of Eqn (3.10) and those of the equal stress (Eqn (3.8)) and Eshelby models for both PMCs and MMCs. It can be seen that the Halpin–Tsai expression represents a fairly good approximation to the axial shear modulus (G_{12}). A striking feature of both the transverse and the shear moduli for polymer matrix composites (Figs 3.4(a) and 3.5(a)) is that they are close to the matrix values up to relatively high fibre volume fractions, although in both cases the true modulus is not as low as the prediction of the equal stress model.

3.3.2 Poisson Ratios

The Poisson ratio ν_{ij} refers to loading in the i direction and is defined as

$$\nu_{ij} = -\frac{\varepsilon_j}{\varepsilon_i} \quad (3.11)$$

For a uniaxially aligned fibre composite, there are three different Poisson ratios, as illustrated in Fig. 3.6.

This brings the total number of elastic constants identified so far for this type of material to seven. However, as outlined in Chapter 4, only five independent elastic constants are needed to describe the behaviour of such a transversely isotropic material. It follows that there must be relationships between these seven values. One of these is the so-called ‘reciprocal relationship’, which is derived in Chapter 4 and may be written

$$\frac{\nu_{12}}{E_1} = \frac{\nu_{21}}{E_2} \quad (3.12)$$

Estimation of the ν_{ij} values using the slab model presents difficulties because of the greater degree to which the Poisson strains of the two constituents must match when compared with the real composite. The effect of this is that, although three Poisson